Coordination Chemistry Reviews, 130 (1994) 1–62

Homo- and heteroatomic chalcogen rings

Risto S. Laitinen and Pentti Pekonen

Department of Chemistry, University of Oulu, Linnanmaa, FIN-90570 Oulu (Finland)

Reijo J. Suontamo

Department of Chemistry, University of Jyväskylä, PO Box 35, FIN-40351 Jyväskylä (Finland)

(Received 23 November 1992; accepted 4 December 1992)

CONTENTS

ABSTRACT

This review describes recent progress in the chemistry of homo- and heterocyclic chalcogen species summarizing their preparation, structural characterization, bonding, and spectroscopic properties. Although it is possible to prepare stoichiometrically pure chalcogen rings, many reactions result in the formation of complicated mixtures. The crystal and molecular structures of many homocyclic rings are known. All heterocyclic rings, however, are disordered and therefore it has not been possible to determine accurate bond parameters for them. The identification of individual molecular species and the composition of mixtures of chalcogen ring molecules have been studied successfully with HPLC and Raman spectroscopy, as well as with ^{77}Se and ^{125}Te NMR spectroscopy. With development of computing techniques, it has been possible to perform MO calculations with increasing sophistication. They have yielded reliable predictions on ground state geometries and electronic structures of different chalcogen rings. The emphasis of research in recent years has shifted from purely structural studies towards understanding the facile interconversion reactions that take place

---

Correspondence to: R.S. Laitinen, Department of Chemistry, University of Oulu, Linnanmaa, FIN-90570 Oulu, Finland.

0010-8545/94/$26.00

between the different chalcogen rings. The experimental and theoretical evidence on the mechanism of these ring interconversion pathways are discussed.

A. INTRODUCTION

Chalcogen elements sulfur, selenium, and tellurium have a strong tendency to catenate, i.e. to form molecular species containing cumulated homo- and heteronuclear chalcogen–chalcogen bonds (for two general reviews of the Group 16 elements, see Refs. 1,2). All three elements exhibit allotropy consisting of both cyclic and open chain molecular forms. Many main group and transition metal compounds and ions also contain polychalcogen fragments. Catenation of chalcogen elements in different chemical environments is summarized in Table 1 with some illustrative examples.

The structural chemistry of homocyclic sulfur species is particularly extensive and has been reviewed several times during the last 10 years [3–6]. There is a growing interest in the research of elemental sulfur, since the tightening environmental control has resulted in significant increase in its production. The flexibility of the S–S bond to adapt to

TABLE 1

Illustrative examples on the catenation of the chalcogen elements (see [1–27])

(A) Allotropes	
Homocyclic species	S_n ($n = 6$–), Se_n ($n = 6$–8), Te_n ($n = 8$)
Polymeric species	S_∞, Se_∞, Te_∞
(B) Interchalcogen compounds	
Heterocyclic species	Se_nS_m, Te_nS_m, Te_nSe_m, $Te_nSe_mS_p$
Interchalcogen polymers	($n + m + p = 6$–8, 12)
(C) Chalcogen-containing compounds	
Homocyclic chalcogenides with exocyclic groups	S_nO ($n = 5$–), etc.
Heterocyclic chalcogenides	$(CH_2)_nS_{6-n}$, $(CH_2)_nSe_mS_{6-n-m}$, S_4N_2, $S_n(NH)_{8-n}$, etc.
Acyclic chalcogenides	R_2S_n, R_2Se_n, R_2Te_n (R = H, F, Cl, alkyl, aryl, etc.), $(SN)_n$, etc.
Transition metal chalcogenides	$[Ti(C_5H_5)_2S_5]$, etc.
(D) Cations	
Homocyclic cations	S_n^{2+}, Se_n^{2+} ($n = 4, 8, 10$, etc.), Te_6^{4+}, etc.
Homocyclic cations with exocyclic groups	S_7I^+, Se_6I^{2+}, etc.
Heterocyclic cations	$Se_nS_{4-n}^{2+}$, $Te_nSe_{6-n}^{2+}$, $Se_nS_{3-n}Cl^+$, etc.
Acyclic cations	$(CH_3S)_3^+$, $(CH_3Se)_3^+$, etc.
(E) Anions	
Homocyclic anions	Se_{10}^{2-}, Se_{11}^{2-}, Te_7^{2-}
Heterocyclic anions	
Acyclic anions	S_n^{2-}, Se_n^{2-}, Te_n^{2-}, $(O_3S)S_n(SO_3)^{2-}$, etc.

different chemical surroundings as well as the ease of its cleavage and formation renders sulfur an attractive and cheap raw material for new applications. Indeed, the research interest in the chemistry of elemental sulfur is shifting from purely structural investigations towards the study of interconversion reactions between the different molecular species.

The allotropy of selenium and tellurium is simpler than that of sulfur (for the previous recent reviews in the structural chemistry of homocyclic selenium molecules, see Refs. 5, 7–9). Although the molecular structures of the selenium- and tellurium-containing species are often similar to those of the analogous sulfur compounds, there are also pronounced differences among the three chalcogen elements. For instance, selenium and tellurium have weaker ability to form homocyclic molecules than sulfur. In fact, the polymeric trigonal chains of selenium and tellurium are the most stable forms of the two elements. However, Se_6, Se_7, and Se_8 ring molecules are known for selenium and have similar molecular structures as analogous sulfur species. In the case of tellurium, the existence of Te_8 has been suggested but not confirmed. The impetus in the study of elemental selenium and tellurium centers on their semi- and photoconducting properties requiring structural characterization of their molecular forms as well as information on their interconversion pathways.

The chemical and structural similarity of the three chalcogen elements has led to investigations on the structures and properties of the binary and ternary systems. There are some recent reviews on the binary selenium sulfides [5,9–12]. Because of the close similarity between sulfur and selenium, the latter can be introduced into the sulfur system as a chemical label. Heterocyclic selenium sulfides can therefore serve as model compounds to study the structural and chemical properties of either sulfur or selenium molecules. Selenium sulfides also bridge the properties of an electrical insulator (sulfur) and a semiconductor (selenium). The heterocyclic tellurium-containing species are much sparser, and therefore very little is known about their properties.

In addition to electrically neutral all-chalcogen homo- and heterocyclic species, many related compounds containing chalcogen–chalcogen bonds are known. It is well established that sulfur, selenium and tellurium can be oxidized to form cyclic cations with or without exocyclic halogen atoms [4–9,13–15] and it has been found very recently that selenium and tellurium can also form cyclic anions [16–19]. When the chalcogen rings are oxidized with trifluoroperoxyacetic acid, homocyclic species with exocyclic oxygen is formed [4–6,9,20–22]. Heterocyclic chalcogen rings are also found in transition metal complexes with the polychalcogenide acting as a chelating ligand [23–27]. Many of the transition metal polychalcogenides can be used as precursors for cyclic chalcogen molecules.

The present review describes the preparation, identification, and structural characterization of homo- and heterocyclic chalcogen molecules as well as advances made in the study of their interconversion pathways. The emphasis is on recent progress, but for the convenience of the reader, older literature is also cited when appropriate.

B. PREPARATION OF CHALCOGEN RINGS

Sulfur is an abundant element in nature occurring in the Earth's crust both as a free element and as sulfide minerals. Crude oil contains organic sulfides, and natural gas contains hydrogen sulfide. It is well known that cyclooctasulfur S_8 is the thermodynamically stable molecular form in NTP (see for instance Ref. 28). All other homocyclic sulfur molecules are only metastable and revert eventually to S_8. Sulfur is manufactured from natural deposits by Frasch and Claus processes followed by various purification processes as have been described previously [4,6,28]. Elemental selenium and tellurium are much less abundant in nature and occur normally together with sulfur in the sulfide ores. They are manufactured during the refinement of the metal [29].

There are several synthetic laboratory routes to produce cyclic chalcogen molecules of different ring sizes as summarized in Table 2. Although some reactions result in the formation of pure stoichiometric compounds, mixtures of different molecular species are produced in many cases. The isolation of individual molecular species may sometimes be based on the differences in solubility or carried out using preparative HPLC. The identification of chalcogen molecules in the mixtures is discussed in the following sections.

Three crystalline forms are known for cyclooctasulfur [94,99–102]. The thermodynamically stable orthorhombic α-S_8 is the eventual end-product in all reactions producing elemental sulfur. It is readily formed upon crystallization of sulfur in CS_2. Monoclinic β-S_8 is stable above 95.4°C [3–6,101,102] and is formed when liquid sulfur solidifies at 115°C. Monoclinic β-S_8 is most conveniently formed upon spontaneous decomposition of copper(I)ethylxanthate in pyridine solution [94].

There are three crystalline forms of cyclic Se_8 [35,36,97,98,103,104]. Monoclinic α- and β-selenium are conveniently obtained by extracting and crystallizing amorphous selenium with CS_2 [7–9,35–38]. After crystallization, the two forms must be manually separated under a microscope. Se_6 is also formed upon crystallization [39]. The third form of Se_8, monoclinic γ-selenium is formed upon the decomposition of $Se_4(NC_5H_{10})_2$ in CS_2 [97,98].

Homo- and heterocyclic chalcogen molecules can be produced from the melts of the elements or element mixtures (see Table 2). Melting is followed by quenching in liquid nitrogen or in an ice bath and by extraction of the melts using non-polar solvents (usually CS_2). When possible, the product mixtures are purified by fractional crystallization.

The condensation reactions of chalcogen hydrides and chlorides provide for the controlled preparation of chalcogen rings [57–63,65]. The method is particularly useful for producing a variety of homocyclic sulfur molecules. The ring size is adjusted by selecting a suitable chain length for the starting sulfanes H_2S_n and chlorosulfanes S_mCl_2. It was initially thought that HCl is needed to catalyze the reactions of longer chlorosulfanes [57], but this has later proved to be unnecessary [105]. In principle, it should also be possible to prepare homocyclic selenium rings using H_2Se and Se_2Cl_2, but there is no

TABLE 2

Laboratory preparation of chalcogen rings[a]

Reaction	Products	Ref.
Molten elements:		
(a) Sulfur	S_n ($n = 7,8,12,18,20$)	28–34
(b) Selenium	Se_n ($n = 6–8$)	35–41
(c) Sulfur-selenium	Se_nS_{8-n}	42-48
(d) Sulfur-tellurium	Te_nS_{8-n}	43,49,50
(e) Selenium-tellurium	Se_nTe_{7-n}, Se_nTe_{8-n}	51,52
(f) Sulfur-selenium-tellurium	Se_nS_{8-n}, Te_nS_{8-n}, $SeTeS_6$	50,53
Reactions of SeO_2		
(a) With SO_2 or N_2H_4	Se_n	54
(b) With H_2S	Se_nS_{8-n}	55
(c) With R–CS–NH–CH_2–C_6H_5	Se_nS_{8-n}	56
Reactions of S_mCl_2:		
(a) With H_2S_n	S_{n+m} (S_6, S_{10}, S_{12}, S_{18}, S_{20})	57–61
(b) With H_2Se	Se_nS_{8-n}	62,63
(c) With KI	S_n ($n = 6$–)	64
Reactions of Se_2Cl_2		
(a) With H_2S_n	Se_nS_{12-n}	65
(b) With KI	Se_6, Se_8	8
Reactions of S_mCl_2/Se_2Cl_2 mixtures with KI	Se_nS_{8-n}	66–68
Reactions $SeCl_4$ with H_2S_n	Se_nS_{8-n}	65
Reactions of $TeCl_4$ ($TeBr_4$) with H_2S_n	Te_nS_{8-n}	69
	Cl_2TeS_7 (Br_2TeS_7)	70,71
Reactions of [$TiCp_2S_5$]:		
(a) With S_nCl_2	S_{5+n} (S_6, S_7, S_9, S_{11}, S_{12}, S_{13})	72–76
(b) With SO_2Cl_2	S_{10}, S_{15}, S_{20}	72,77–80
(c) With Se_2Cl_2	1,2-Se_2S_5, SeS_5, 1,2,3-Se_3S_5	81,82
(d) With Se_xBr_2	SeS_5, 1,2-Se_2S_5, 1,2,3-Se_3S_5, Se_2S_{10}	83
(e) With Se_2Cl_2/S_2Cl_2	Se_nS_{7-n}, Se_nS_m	68
(f) With SeS_5SeCl_2	1,7-Se_2S_{10}	84
Reactions of [$TiCp_2Se_5$]:		
(a) With Se_2Cl_2	Se_7	85
(b) With SCl_2	Se_5S	85
(c) With S_2Cl_2	1,2,3,4,5-Se_5S_2	85,86
Reactions of [$TiCp_2Se_nS_{5-n}$] with Se_2Cl_2 or S_2Cl_2	Se_xS_{7-x}	87

TABLE 2 (*continued*)

Reaction	Products	Ref.
Reactions of [$TiCp_2(\mu\text{-}S_2)_2TiCp_2$]:		
(a) With S_nCl_2	S_n (S_6, S_7, S_8, S_{10}, S_{15}, S_{20})	88
(b) With Se_2Cl_2	1,2,5-Se_3S_4, 1,2,5,6-Se_4S_4	88
Reactions of [$TiCp_2(\mu\text{-}Se_2)_2TiCp_2$]		
(a) With S_2Cl_2	1,2,5-Se_3S_4, 1,2,5,6-Se_4S_4	88–90
(b) With Se_2Cl_2	Se_8	88
Reactions of [$TiCp_2(\mu\text{-}Se_nS_{2-n})_2TiCp_2$] with S_2Cl_2 or Se_2Cl_2	Se_nS_{8-n}	91
Reaction of [$TiCp_2(\mu\text{-}Te_nS_{2-n})_2TiCp_2$] with S_2Cl_2	TeS_7, 1,2-Te_2S_6	92
Reactions of [$TiCp_2(CO)_2$]:		
(a) With S_6/S_nCl_2	S_{8+n} (S_9, S_{10})	93
(b) With S_8/S_nCl_2	S_{5+n}	93
Miscellaneous reactions:		
(a) Decomposition of $CuSSCOC_2H_5$	Monoclinic γ-S_8	94
(b) Reaction of $Na_2S_2O_3$(aq) with HCl(aq)	S_6, S_7, S_8	95,96
(c) Reaction of $Se_4(NC_5H_{10})_2$ with CS_2	Monoclinic γ-Se_8	97,98
(d) Oxidation of S_6 or S_7 with CF_3COOOH	S_{10}	77,78

[a] Early literature has been discussed in refs. 3–12.

published information about the reaction. It is possible that polymeric hexagonal α-selenium is formed in the reaction. Hydrogen selenide and chlorosulfanes [62,63] and sulfanes with dichlorodiselane [65] produce mixtures of cyclic selenium sulfides.

Transition metal chalcogenides of the type [$TiCp_2E_5$] and [$TiCp_2(\mu\text{-}E_2)_2TiCp_2$] (E = S, Se; Cp = $C_5H_5^-$ or its alkyl substituted derivative) are also useful reagents for the preparation of both homo- and heterocyclic chalcogen rings. The reaction of [$TiCp_2S_5$] with $SnCl_2$ results in the formation of S_{n+5} ring molecules [72–76]. Cyclodecasulfur S_{10} is formed together with small amounts of S_{15} and S_{20} when [$TiCp_2S_5$] reacts with SO_2Cl_2 [72,77–80]. Upon reaction with Se_2Cl_2 a seven-membered heterocycle 1,2-Se_2S_5 is formed [82]. It quickly equilibrates in CS_2 solution to SeS_5 and 1,2,3-Se_3S_5 accompanied by small amounts of twelve-membered selenium sulfide rings Se_nS_{12-n} [81–83]. It has recently been observed that $SeSCl_2$ can be obtained by mixing S_2Cl_2 and Se_2Cl_2 [68,106]. The reaction of this mixture with [$TiCp_2S_5$] affords expectedly S_7, SeS_6, and 1,2-Se_2S_5 as the main products [68]. 1,2-Se_2S_5 can be chlorinated to form SeS_5SeCl_2 [84]. Its reaction with [$TiCp_2S_5$] produces 1,7-Se_2S_{10}.

The reactions of $[TiCp_2Se_5]$ are similar to those of $[TiCp_2S_5]$. The range of products is limited by the availability of chloroselanes of different chain lengths. The reactions with SCl_2, S_2Cl_2, and Se_2Cl_2 produce pure stoichiometric Se_5S, 1,2,3,4,5-Se_5S_2, and Se_7, respectively [85,86]. The reaction of $[TiCp_2Se_nS_{5-n}]$ mixtures with S_2Cl_2 or Se_2Cl_2 also results in the formation of seven-atomic selenium sulfide ring molecules with relative amounts expected from the composition of the starting mixtures [87].

Dinuclear $[TiCp_2(\mu\text{-}E_2)_2TiCp_2]$ (E = S, Se) may be formed either by dechalcogenization of $[TiCp_2E_5]$ [108] or by reducing the chalcogen element with $LiBHEt_3$ and treating the resulting suspension with $[TiCp_2Cl_2]$ in an analogous manner to the preparation of mononuclear $[TiCp_2E_5]$ [108,109] The main reaction product is controlled by the molar ratio of $[TiCp_2Cl_2]$ and chalcogen. $[TiCp_2(\mu\text{-}E_2)_2TiCp_2]$ also reacts with chalcogen chlorides to form chalcogen rings as shown in Table 2. For instance, $[TiCp_2(\mu\text{-}Se_2)_2TiCp_2]$ and S_2Cl_2 form 1,2,5,6-Se_4S_4 [88,89]. Steudel et al. [88] have observed that the reaction also produces a seven-membered selenium sulfide 1,2,5-Se_3S_4. It is interesting to note that the reaction of $[TiCp_2(\mu\text{-}Se_2)_2TiCp_2]$ with S_2Cl_2 results in the formation of identical products. The reaction of $[TiCp_2(\mu\text{-}Se_2)_2TiCp_2]$ with SCl_2 or S_2Cl_2 in the molar ratio 1:1 was reported to produce $[TiCp_2Se_3S_2]$ (selenium atoms in positions 2, 4 and 6) and $[TiCp_2Se_4S]$, respectively [90]. The treatment of these two titanocene compounds with chlorosulfanes and chloroselanes provides new routes to heterocyclic selenium sulfides.

It is also possible to prepare mixed dinuclear complexes with the two bridges containing different chalcogen elements [91,92]. The reactions of $[TiCp_2(\mu\text{-}Se_nS_{2-n})_2TiCp_2]$ with SCl_2, S_2Cl_2 and Se_2Cl_2 yield a variety of Se_nS_m molecules with their identity and relative amounts consistent with the composition of the original mixture of the dinuclear complexes [91].

The reaction of dichlorodisulfane with potassium iodide produces mainly S_8 and S_6 with smaller amounts of S_{12}, S_{18} and S_{20} [64]. Dichlorodiselane reacts in the analogous manner and yields Se_6 and Se_8 [8]. Heterocyclic selenium sulfide mixtures can be prepared by using mixtures of dichlorodiselane and dichlorodisulfane [66–68]. All these reactions probably proceed via formation of unstable chalcogen iodides.

Literature on homo- and heterocyclic tellurium-containing species is rather sparse. The existence of cyclic Te_8 in zeolite matrices has been suggested [110,111], but not unambiguously confirmed. The formation of binary Te_nS_{8-n} in the sulfur-rich sulfur-tellurium melt has been demonstrated by X-ray crystallographic [43], mass spectrometric [49] and ^{125}Te NMR spectrometric [50] studies. The last may also indicate the presence of small amounts of Te_8 in the sulfur tellurium melt. NMR spectroscopic observations also show the existence of 1,2-$TeSeS_6$ in the ternary sulfur-selenium-tellurium melt. Nagata et al. [51,52] have succeeded in crystallizing disordered Te_nSe_{7-n} and Te_nSe_{8-n} phases from the selenium-tellurium melt. Tellurium tetrachloride and tetrabromide react with hydrogen sulfide to produce Te_nS_{8-n} [69], Cl_2TeS_7 and Br_2TeS_7 [70,71]. The reaction utilizing $[TiCp_2(\mu\text{-}Te_nS_{2-n})_7TiCp_2]$ and S_2Cl_2 has recently been shown to produce TeS_7 and 1,2-Te_2S_6 [92].

C. BONDING CHARACTERISTICS OF THE CHALCOGEN RINGS

Chalcogen–chalcogen bonds are very flexible and adapt themselves to many different chemical surroundings. The general properties of sulfur–sulfur bonds have been reviewed by Meyer [112] and Steudel [113]. It is now generally believed that the bond parameters observed in polymeric sulfur, selenium and tellurium best represent the unstrained chalcogen–chalcogen bonds. The experimental bond geometries are presented in Table 3. The torsion angle of near 90° has been explained in terms of the mutual interaction of the p lone-pair orbitals of the neighboring chalcogen atoms. The slight deviation from 90° can be explained by taking into account the interaction between the atoms i and $i+2$ (for example, see the discussion in Ref. 113). Recent ab initio crystal orbital (CO) calculations [118] on the torsional potential in sulfur helices and density functional studies on the energy surfaces of polymeric sulfur and selenium [119] yield geometrical parameters that are in agreement with experimental values. A variety of ab initio MO calculations of disulfane and other dichalcogen hydrides at different levels of sophistication also reproduce the bond geometry of a single chalcogen–chalcogen bond [120–122 and refs. therein] . However, there is experimental information available only for HSSH. The microwave spectroscopic determination of the molecular structure and the experimental rotational barriers [123 and refs. therein] are in agreement with the values obtained from the MO calculations.

The structural and electronic features of the different chalcogen–chalcogen bonds are rather similar [121,122] as exemplified by the ab initio MO energy diagrams of all members in the $HSe_nS_{3-n}H$ series shown in Fig. 1. The valence orbitals seem to be rather insensitive to the substitution of sulfur by selenium or vice versa. This is further emphasized by the fact that the calculated energy change to form two S–Se bonds from one S–S and one Se–Se bond is very small [121,122], in good agreement with the enthalpy of mixing of liquid sulfur and selenium [124] or with the enthalpy change in the reaction of gaseous S_2 and Se_2 to form SeS(g) [125]. The electronic structures of the chalcogen hydrides involving tellurium seem to be somewhat more different [122].

Cyclic chalcogen molecules show very similar bond parameters to the polymeric chalcogen chains. This leads to the existence of puckered ring molecules as shown in Table 4. It is readily seen that, in the solid state, the molecules having the same ring size

TABLE 3

Bond parameters in polymeric sulfur, selenium, and tellurium

Species	Bond length (pm)	Bond angle (°)	Torsion angle (°)	Ref.
Sulfur	206.6	106.0	85.3	112[a]
Selenium	237.3	103.1	100.7	116
Tellurium	283.4	103.1	100.6	117

[a] Meyer [112] has based the estimation on the diffraction data of Lind and Geller [114,115].

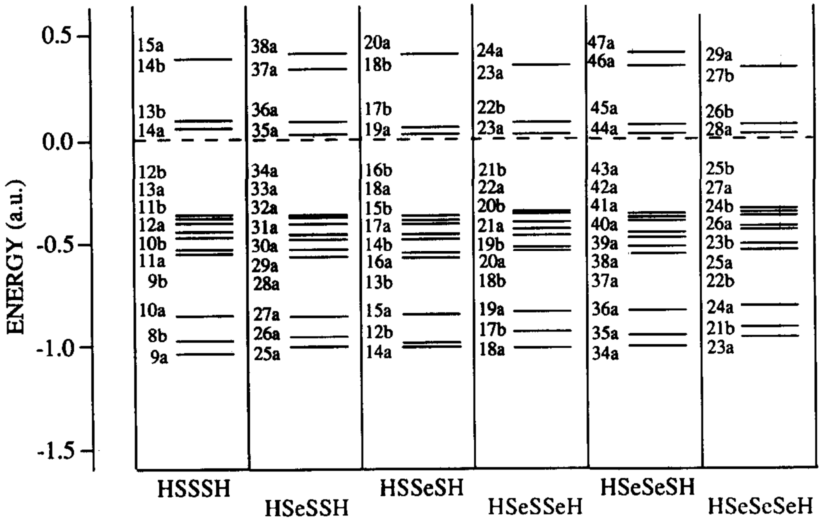

Fig. 1. The orbital energies of $HSe_nS_{3-n}H$ (n = 0–3) [121] (© Elsevier Science Publishers).

show similar molecular geometries regardless of the chemical identity of the chalcogen atoms.

In the following, the structures, bonding characteristics and spectroscopic properties of the different chalcogen rings are described according to their ring sizes. The experimental observations are complemented by the theoretical studies, where appropriate.

D. EIGHT-ATOMIC RING MOLECULES

(i) Sulfur

All three polymorphs of cyclooctasulfur consist of puckered crown-shaped molecules with an idealized point group D_{4d} as shown in Table 4 [94,99–102]. The bond parameters in each polymorph are rather similar. The crown-shaped eight-membered sulfur ring is also found in many adducts as exemplified by $CHI_3 \cdot 3S_8$ [142], $SbI_3 \cdot 3S_8$ [143], $[Cu(phen)_2I]I \cdot S_8$ [144], $SnI_4 \cdot 2S_8$ [145], $(PPh_4)_4[Ag_2S_{20}] \cdot S_8$ [146], $\{N(PPh_3)_2\}[Ag(S_9)] \cdot S_8$ [147], $[Ag(S_8)_2](AsF_6)$ [148], $[WCl_6] \cdot S_8$ [149] and $[WCl_4S] \cdot S_8$ [150].

Coppens et al. [99] have reported the charge distribution in orthorhombic α-S_8 on the basis of low temperature crystal structure determination by X-ray and neutron diffraction. Their data indicate that, along the S–S bond, the electron density has a complicated double maxima distribution with remarkably small electron surplus at the midpoint of the S–S bond. Evidence was also obtained for a p lone-pair orbital of sulfur perpendicular to the bonding plane. The SCF-Xα-SW calculations of Salahub et al. [151] and the density functional approach of Hohl et al. [152] were able to reproduce qualitatively

TABLE 4

The molecular structures of the chalcogen rings in the solid state

Molecule	Example	Ref.
	S_6	126,127
	Se_6	128
	Se_5S	85
	S_7	129,130
	Se_7[a]	
	Se_5S_2	85
	Te_nSe_{7-n}	52
	S_8	94,99–102
	Se_8	35,98,103,104
	Se_nS_{8-n}	47,55,81,89,133–136
	Te_nSe_{8-n}	51
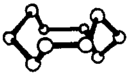	S_{10}	78,137
	S_{11}	75,138
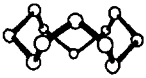	S_{12}	76,139
	Se_nS_{12-n}	65
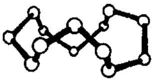	S_{13}	75
	S_{18}	60,140,141
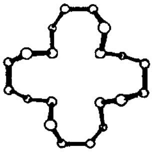	S_{20}	60,61

---

[a] There is no reported crystal structure for Se_7, but the molecule is found in two ionic products $[Na(12\text{-crown-}4)_2^+]2Se_8^{2-}\cdot(Se_6,Se_7)$ [131] and $(NEt_4^+)_2[Se_5^{2-}\cdot 1/2Se_6\cdot Se_7]$ [132]. The structure and conformation of Se_7 in these two compounds is similar to that of S_7 [129,130].

the experimental charge distribution. The latter could even estimate the lone-pair density as well as the double maximum distribution along the S–S bond [152].

The multiple temperature single crystal X-ray diffraction study of monoclinic β-sulfur has revealed that there is an order-disorder transition at 198 K [102]. Above the transition temperature, one-third of the molecules is disordered, there being two possible orientations for these molecules in the lattice (see also [101]). The ordering energy is estimated to be ca. 5 kJ mol^{-1} with the upper limit for the barrier between the two sites ca. 21 kJ mol^{-1}. A simple pathway has been suggested for the transformation mainly consisting of an independent molecular rotation. The calculated energy surface in the vicinity of the two minima is consistent with the crystallographic thermal motion.

Theoretical calculations have been performed to predict the molecular geometry and electronic structure of S_8. The molecular mechanics method has been applied to several homocyclic species [153]. Small sulfur molecules have also been studied by the Hückel method [154–157] and there are several semi-empirical calculations [157–175] with special emphasis on the interpretation of the photoelectron [157,163,164,175–178] or optical absorption [156,165,166,178,179] spectra and on the estimation of the formation energetics [167–172]. The SCF-Xα-SW MO technique has been applied, in addition to the electron deformation density distribution study described above, to the investigation of the structural changes in small sulfur rings on oxidation and reduction [180]. Richardson and Weinberger [178] interpreted their UPS, XPS and UV-absorption spectra with the help of SCF-Xα-SW calculations.

With the development of computational techniques it has also become possible to perform more extensive ab initio molecular orbital calculations at various levels of sophistication for cyclooctasulfur [120,181–191]. The degree of agreement between the calculated and observed geometrical parameters depends on the level of sophistication of the method. Some recent ab initio geometries are listed in Table 5. It is well known that with the exception of the STO-3G basis set, the correct prediction of the bond parameters requires 3d-polarization functions as clearly demonstrated by Hinchliffe [192] and Marsden and Smith [193] for the S–S bond of H_2S_2. It is seen from Table 5 that with a flexible basis set, the agreement between the calculated and experimental geometry of S_8 is excellent.

Birner et al. [120] have estimated the ring strain by comparing the total energy of the S_8 molecule with that obtained by considering the energy increment per sulfur atom in polysulfanes. They concluded that the cyclooctasulfur ring is practically strainless. This is in agreement with the earlier semi-empirical calculations of Baird [168] and verifies the original suggestion of Benson [194].

Molecular dynamics simulation has proved to be an effective technique to study the structural chemistry of sulfur in the molten state [195–197]. The combination of density functional formalism with local density approximation for the exchange-correlation energy and molecular dynamics with simulated annealing techniques yields a parameter-free method for calculating the ground-state geometries and electronic properties of the molecules (for general description of the method, see refs. 198–202 and references

TABLE 5

The calculated equilibrium geometry of S_8 (D_{4d})

Parameter	STO-3G[a]	MB(Pseudo)[b]	DZ[a]	DZP[a]	DZP[c]	3-21G*[d]	DPZ(Pseudo)[e]	DFSA[f]	Expt.[g]
r (pm)	207.3	228.9	224.0	207.0	206.0	205.2	206.1	206.4	202.3–206.0
α (°)	103.8	103.2	104.7	106.8	107.2	107.1	106.8	108.5	105.8–109.0
τ (°)	103.3	103.9	102.4	100.1	99.7	99.8	100.2	98.1	96.4–101.3

[a] Ref. 190. The earlier STO-3G geometry of Carlson and Pedersen [181] is virtually identical to the one reported here. The DZ basis is (11s7p/6s4p) and the DZP basis S(11s7p1d/6s4p1d).

[b] Ref. 186.

[c] Ref. 187. The DZP basis is S(12s8p1d/5s3p1d).

[d] Refs. 188 and 189.

[e] Ref. 120.

[f] Ref. 203.

[g] Refs. 93,99–102.

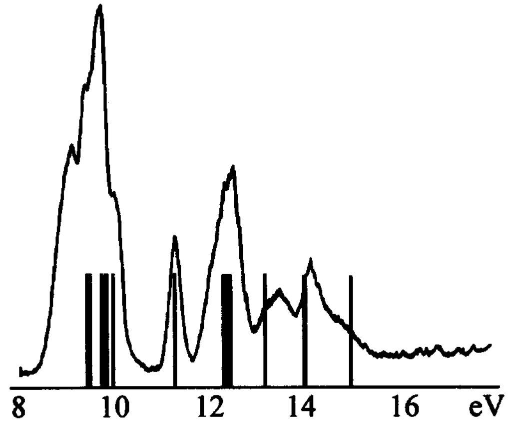

Fig. 2. Comparison of the He(I) photoelectron spectrum of S_8 [176] with the ground-state eigenvalue spectrum calculated using MD DF techniques [152]. The vertical lines indicate the energies of the molecular orbitals in the p band (© American Institute of Physics).

therein). Hohl et al. [152] have applied the method for sulfur rings S_3–S_{13}. The agreement between the calculated and the experimental geometries for S_8 [203] is shown in Table 5. The calculated eigenvalue spectrum of S_8 also reproduces the He(I) photoelectron spectrum of sulfur vapor at 413 K (see Fig. 2) in a satisfactory manner. Jones and Hohl [203] have shown that in addition to the D_{4d} isomer of S_8 there is another isomer that lies ca. 42 kJ mol^{-1} higher in energy. This isomer has a molecular symmetry of C_2 and shows alternation in bond lengths and torsional angles. The two isomers of S_8 are shown in Fig. 3. They serve as models for all different cyclic chalcogen species, since rings with high symmetry (e.g. E_6, E_8, E_{10}, E_{12}, etc.) show only small or no alternation in the bond lengths and torsion angles, while the alternation in both the bond lengths and torsional angles is significant in molecules with low symmetry (e.g. E_7, E_9, E_{11} etc.).

There are several reports of vibrational spectra of S_8 and the force-field calculations have been performed for the assignment of the fundamental vibrations. The main features of the vibrational spectra of S_8 and other homocyclic sulfur molecules have been reviewed several times [3–6]. The fundamental vibrations calculated with various ab ini-

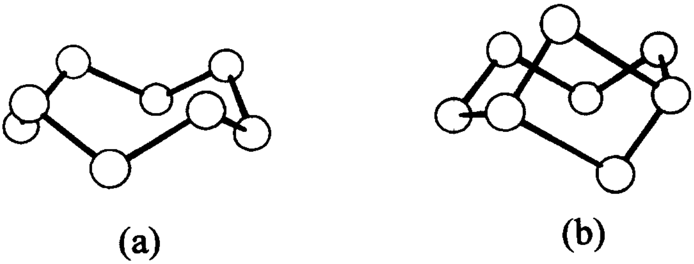

Fig. 3. Two possible isomers of S_8 and Se_8. (a) D_{4d} structure, (b) C_2 structure [203].

tio MO approaches at different levels of theory provide a qualitative agreement with the experimental values [120,187–190]. Gramaccioli and Filippini have carried out a lattice-dynamical calculation for orthorhombic S_8 with a non-rigid model for molecular bodies [204]. Venutti et al. [205,206] report a molecular dynamics simulation of the crystalline S_8 and apply the model in the prediction of molecular vibrations. Recently, Chang et al. [207] and Harvey and Butler [208] have recorded the Raman spectrum of S_8 at 10 K and 40 K, respectively, and discussed the assignment of the new features. Wang et al. [209], Wolf et al. [210] and Nagata et al. [211] have studied orthorhombic S_8 under pressures up to ca. 10 GPa and found a reversible phase change at 5–6 GPa. The high-pressure phase was suggested to be composed of sulfur chains [210,211]. Raman spectroscopy has also been used in the identification of molecular species in sulfur vapor [212,213]. The utilization of Raman spectroscopy in the analysis of molecular mixtures of elemental sulfur is discussed in more detail below.

(ii) Selenium and tellurium

The molecular structures of the three known crystalline modifications of cyclooctaselenium are similar to cyclooctasulfur (see Table 4) [35,97,98,103,104,209]. The intermolecular distances in all crystalline forms are significantly shorter than the van der Waals' distance as is also the case in S_8 [94,99–102]. However, the intermolecular interactions in Se_8 seem to be stronger than those in S_8 [5,7–9]. This is particularly the case in γ-Se_8 [97,98] where the shortest observed intermolecular distance is actually shorter than in any modification of S_8 [94,99–102].

Due to the obvious computational difficulties, there are very few theoretical calculations on Se_8 comprising mainly a few extended Hückel and semi-empirical studies [165,166,185,215–217]. Up to the present, there are no reports on the ab initio calculations of cyclooctaselenium. The most reliable predictions of molecular geometries of Se_8 and other smaller selenium rings come from the parameter-free density functional calculations of Hohl et al. [218]. The calculated structural parameters [203] ($r_{SeSe} = 235.1$ pm, $\alpha = 107.2°$, $\tau = 99.7°$) are in agreement with the experimental values for Se_8 ($r_{SeSe} = 233.4$–234 pm, $\alpha = 105.7$–$105.8°$, $\tau = 101$–$101.4°$; see [35,97,98,103,104,209]). The density functional calculations of Jones and Hohl [203] indicate that Se_8 has a low-symmetry isomer ca. 39 kJ mol^{-1} higher in energy (see Fig. 3). A similar isomer was also found for S_8.

The vibrational spectrum of Se_8 has been reported several times and assigned on the basis of the force-field calculations (see [8,9] for recent reviews). Nagata et al. have studied the dependence of the solid state Raman spectra of monoclinic α-Se_8 and Se_6 on hydrostatic pressure [219] and recorded the photoconductivity and photoacoustic spectra for all known crystalline allotropes [220]. The results are discussed in terms of intermolecular interaction.

Becker et al. [221–223] have recorded vacuum-UV-photoelectron spectra of elemental selenium and discussed the results in terms of geometries and electronic structures of homocyclic Se_n ($n = 5$–8) molecules. The difference in the 10.0 eV photoelectron spectra of the selenium ring molecules containing even and odd numbers of selenium atoms is obvious in the 4p lone-pair bands shown in Fig. 4 and reflects the differing symmetries of the molecules.

^{77}Se NMR spectroscopy is a powerful technique to study selenium-containing molecular species. The ^{77}Se isotope has a natural abundance of 7.58%, a nuclear spin of 1/2, and a sensitivity of 2.98 relative to that of ^{13}C (for NMR spectroscopic data of ^{77}Se, see for instance [224]). In CS_2 solution at room temperature, Se_8 shows the ^{77}Se NMR signal at 614.6 ppm relative to neat Me_2Se [225,226]. In the spectrum of the molten mixture of

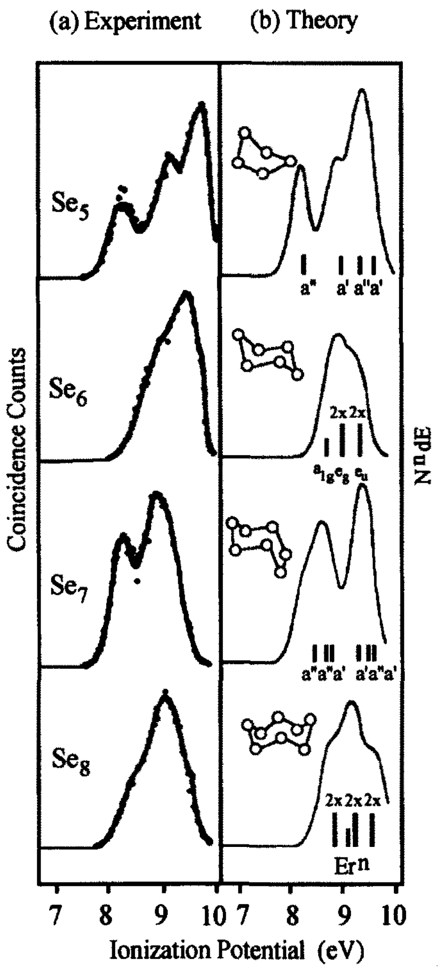

Fig. 4. The comparison between (a) the experimental 10.0 eV photoelectron spectra of Se_5, Se_6, Se_7 and Se_8 and (b) calculated spectra. The MO energy scheme of Ikawa et al. [223 and refs. therein] is also shown (© Verlag der Zeitschrift für Naturforschungen).

sulfur and selenium recorded at 135°C, the resonance due to Se_8 appears at 621 ppm [227]. The signal remains a singlet in the ^{77}Se-enriched sample (enrichment 92%) [225] indicating that the cyclooctaselenium molecule has the symmetry of D_{4d} with all selenium atoms both chemically and magnetically equivalent.

The existence of the Te_8 ring in zeolites has been suggested based on conductivity measurements and Raman spectroscopy [110,111]. This suggestion has not been confirmed, but very recently, in connection with a ^{125}Te NMR spectroscopic study of the sulfur-tellurium and sulfur-selenium-tellurium melts at 145°C (see below for a more detailed discussion), a weak resonance was observed at 848 ppm relative to neat Me_2Te at room temperature, which could be caused by the presence of Te_8 in the melt. [50].

(iii) Heterocyclic chalcogen molecules

The similarity of sulfur and selenium is reflected by a complicated binary system between the two elements. As discussed above, most of the synthetic methods listed in Table 2 produce mixtures of various selenium sulfides. In fact, only the reactions of titanocene compounds of the types $[Ti(C_5H_5)_2E_5]$ and $[Ti(C_5H_5)_2(\mu\text{-}E_2)_2Ti(C_5H_5)_2]$ (E = S, Se) with dichlorosulfanes or dichlorodiselane are known to result in the formation of pure stoichiometric compounds. The eight-membered species Se_nS_{8-n} are the most abundant and most stable molecular species found in the sulfur-selenium mixtures, although HPLC and NMR investigations indicate that many systems also contain heterocyclic selenium sulfides of other ring sizes. The early characterization of the cyclic selenium sulfides has been reviewed several times [9–12].

The 30 possible selenium sulfide rings Se_nS_{8-n} are listed in Table 6 together with the abbreviated notation used below. In addition to the structural isomerism between the rings of the same elemental composition, several molecules are chiral and can in principle exhibit optical isomerism. Theoretically, there are equally many isomers for the binary Te_nS_{8-n} and Te_nSe_{8-n} ring molecules, and for the ternary rings $Te_nSe_mS_y$ $(n+m+y=8)$, there are as many as 414 possible isomers. However, only a few tellurium-containing ring molecules are known.

Several attempts to determine the crystal structure have been made for the binary selenium sulfides Se_nS_{8-n} [47,55,81,89,134–136]. Pupp and Weiss [69] have reported a single crystal X-ray diffraction study of Te_nS_{8-n} and Nagata et al. [52] have determined the crystal structure of the mixed tellurium selenide phase Te_nSe_{8-n}. A preliminary X-ray diffraction of sulfur-rich sulfur-selenium-tellurium phase has indicated that the crystal is isomorphous with orthorhombic α-sulfur and is therefore also composed of eight-atomic ring molecules. All crystal structures reported up to the present have been disordered with different chalcogen atoms randomly distributed over the atomic sites. X-Ray crystallographic studies have therefore only indicated that the overall conformations of the eight-atomic chalcogen heterocycles are similar to those of S_8 [94,99–102] and Se_8 [35,97,98,103,104,209], but the calculation of accurate bond parameters and the identification of individual molecular species have not been possible even in the cases of 1,2,3-

Se_3S_5 [81], 1,2,5,6-Se_4S_4 [89], and Se_7S [136] which are known to be stoichiometrically pure or nearly so.

Vibrational spectroscopy provided the first useful indications of the molecular composition of selenium sulfide mixtures [9–12, 68]. The force constant calculations for selected Se_nS_{8-n} species [228,229] have established that the Se–S stretching region (400–320 cm^{-1}) is sensitive to the chemical environment of the bond. With two cumulated Se–S bonds (the structural unit –S–Se–S–), the vibrational coupling causes large splitting between the symmetric and asymmetric stretching vibrations. When there are two or more adjacent selenium atoms, the Se–S bonds are further separated and the vibrational coupling is smaller and causes the symmetric and asymmetric stretching modes to coincide. The Raman spectra of 1,2,3-Se_3S_5 [81], 1,2,5,6-Se_4S_4 [89] and Se_7S [136] could be assigned on the basis of these force field calculations. The spectra of two former species are shown in Fig. 5.

The Se–S stretching region of the Raman spectra of crystalline Se_nS_{8-n} phases obtained by quenching and recrystallizing the molten mixtures of the elements indicate that both structural units, S–Se–S– and –S–Se$_n$–S– ($n \geq 2$) may be present, but that the latter is more abundant [228]. This conclusion finds support from the observation that the Se–Se stretching vibrations are seen in the Raman spectra of these phases even when the selenium content is low [48,228,230,231], ruling out the report that pure 1,3,5,7-Se_4S_4 could be prepared from sulfur-selenium melt [232]. S_8 and Se_8 are also present in some samples [228]. The spectrum of the crystalline product obtained in the reaction of the Se_2Cl_2–S_2Cl_2 mixture with KI shows two strong bands at 380 and 340 cm^{-1} indicating the presence of –S–Se–S– units in significant abundance [68]. The formation of isolated sel-

TABLE 6

The abbreviated notation for all possible Se_nS_{8-n} ring molecules[a]

SeS_7 **A_1**	1,2-Se_2S_6 **A_2**	1,2,3-Se_3S_5 **A_3**	1,2,3,4-Se_4S_4 **A_4**	1,2,3,4,5-Se_5S_3 **A_5**	1,2,3,4,5,6-Se_6S_2 **A_6**	Se_7S **A_7**
	1,3-Se_2S_6 **B_2**	1,2,4-Se_3S_5 **B_3**	1,2,3,5-Se_4S_4 **B_4**	1,2,3,4,6-Se_5S_3 **B_5**	1,2,3,4,5,7-Se_6S_2 **B_6**	
	1,4-Se_2S_6 **C_2**	1,2,5-Se_3S_5 **C_3**	1,2,3,6-Se_4S_4 **C_4**	1,2,3,5,6-Se_5S_3 **C_5**	1,2,3,4,6,7-Se_6S_2 **C_6**	
	1,5-Se_2S_6 **D_2**	1,3,5-Se_3S_5 **D_3**	1,2,4,5-Se_4S_4 **D_4**	1,2,3,5,7-Se_5S_3 **D_5**	1,2,3,5,6,7-Se_6S_2 **D_6**	
		1,4,6-Se_3S_5 **E_3**	1,2,4,6-Se_4S_4 **E_4**	1,2,4,6,7-Se_5S_3 **E_5**		
			1,2,5,6-Se_4S_4 **F_4**			
			1,2,4,7-Se_4S_4 **G_4**			
			1,3,5,7-Se_4S_4 **H_4**			

[a] Homocyclic S_8 and Se_8 are excluded from the table.

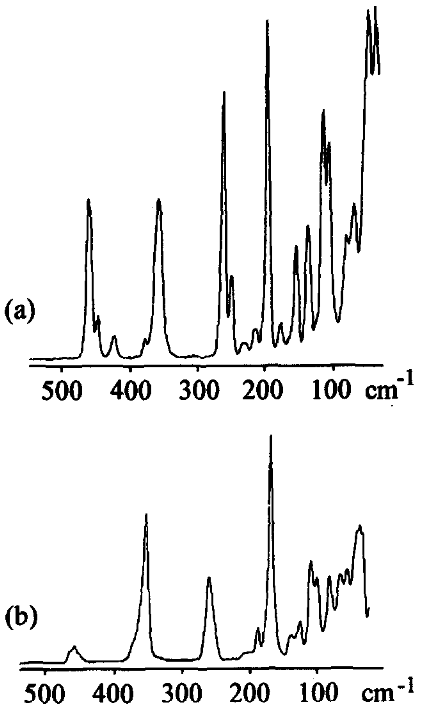

Fig. 5. Low-temperature Raman spectra of (a) 1,2,3-Se_3S_5 [85] (© Johann Ambrosius Barth Verlag) and (b) 1,2,5,6-Se_4S_4 (adapted from [89], © American Chemical Society).

enium atoms in the Se_nS_{8-n} rings have been explained by the formation of $SeSCl_2$ from S_2Cl_2 and Se_2Cl_2 in solution. There is independent mass spectrometric, Raman spectroscopic and ^{77}Se NMR spectroscopic evidence of the equilibrium between $SeSCl_2$, S_2Cl_2 and Se_2Cl_2 [68,106].

^{77}Se NMR spectroscopy is the most powerful technique to date to identify individual selenium sulfides in mixtures of complicated composition [225,226]. The spectral assignment is based on the combined information from the natural-abundance samples and from the samples of the same chemical composition but involving selenium enriched with ^{77}Se-isotope (enrichment 92%). The NMR spectra of the CS_2 solutions from the quenched natural-abundance and ^{77}Se-enriched sulfur-selenium melts both containing 30 mol% of selenium are shown in Fig. 6. The spectrum in Fig. 6(a) is from a natural-abundance sample and that in Fig. 6(b) is from the enriched sample. Due to the low natural abundance of ^{77}Se-isotope, the ^{77}Se–^{77}Se coupling can only be observed by the appearance of small satellites that are often lost in the background. Full coupling information is only obtained when the enrichment of the ^{77}Se-isotope is sufficiently high as exemplified in Fig. 7 showing the details of the splitting patterns and the interpretation of the spectrum in Fig. 6(b). For three-spin systems, the assignment of the resonances is straightforward and could be carried out by visual inspection, but the second order effects become more pronounced in the signals in more extensive spin systems and they have to

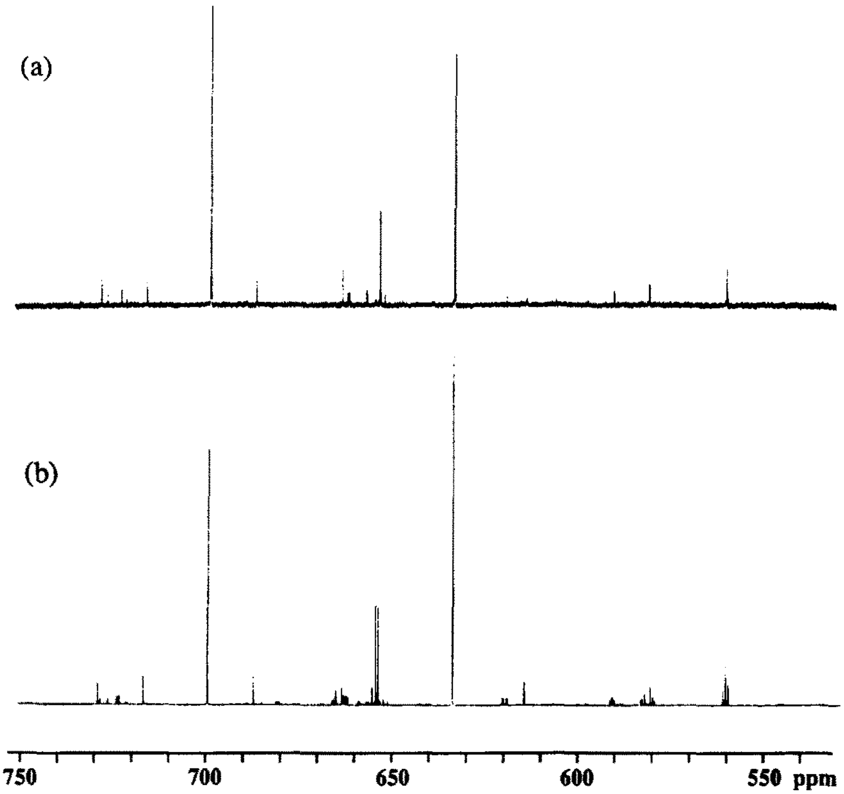

Fig. 6. ^{77}Se NMR spectra of the CS_2 solutions obtained from quenched sulfur-selenium melts containing 30 mol% of (a) natural-abundance selenium, (b) ^{77}Se-enriched-selenium [226] (© American Chemical Society).

be analysed by spectral simulation [226,233]. The observed and calculated transitions of 1,2,3,4-Se_4S_4 (**A_4**) are shown in Fig. 8 and demonstrate the power of ^{77}Se NMR spectroscopy. The low-field multiplet is overlapped by the quartets of 1,2,4- and 1,2,5-isomers of Se_3S_5 (**B_3** and **C_3**). The comparison of the enriched spectrum with the natural-abundance spectrum (see Fig. 6) shows that there are three discrete resonances in this region and thus it is possible to assign all transitions.

There are several NMR resonances in the spectra of Fig. 6 that remain singlets in the ^{77}Se-enriched sample indicating the chemical and magnetic equivalence of the selenium atoms within the ring molecules. These signals were assigned on the basis of the trends in the chemical shifts deduced from unambiguously identified molecular species. These trends are shown in Fig. 9 and can be rationalized in terms of electronegativities of the neighboring atoms [226]. The chemical shifts can roughly be divided into three groups: The selenium atom with two sulfur neighbors shows resonances in the region above 690 ppm. With one selenium and one sulfur neighbor, the signals lie at 690–620 ppm and with two selenium neighbors below 620 ppm. There is a secondary, cumula-

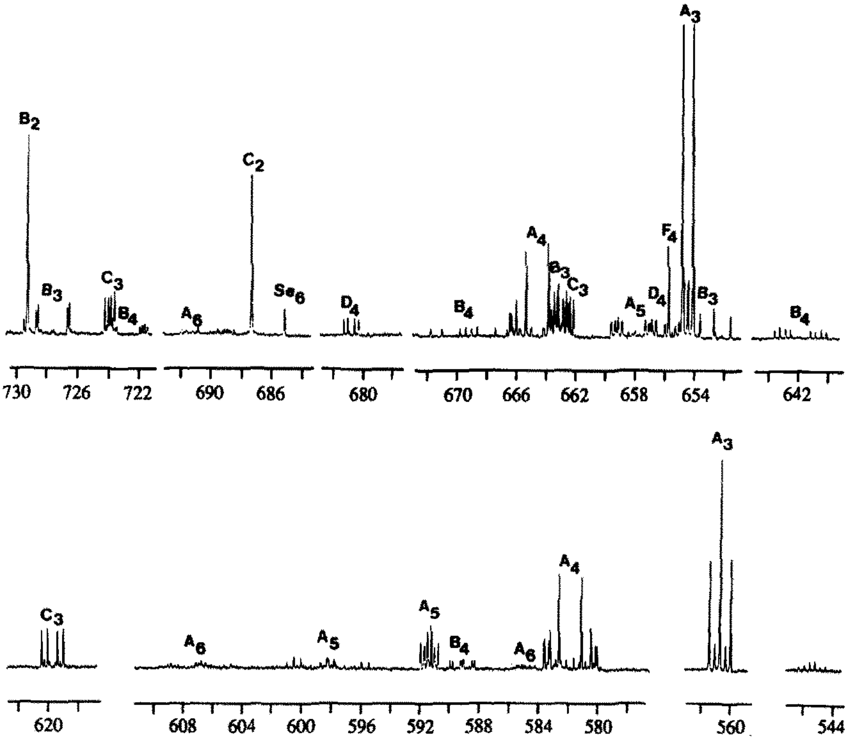

Fig. 7. Details of the coupling patterns of the spectrum in Fig. 6(b) [226] (© American Chemical Society).

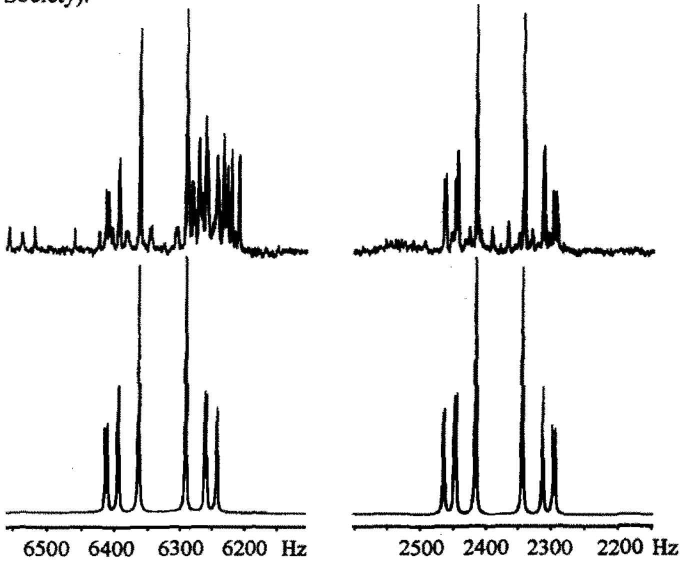

Fig. 8. Observed and calculated spectra of 1,2,3,4-Se_4S_4 (A_4). The small signals in the middle of the two multiplets are caused by the existence of different isotopomers of significant abundance [226] (© American Chemical Society).

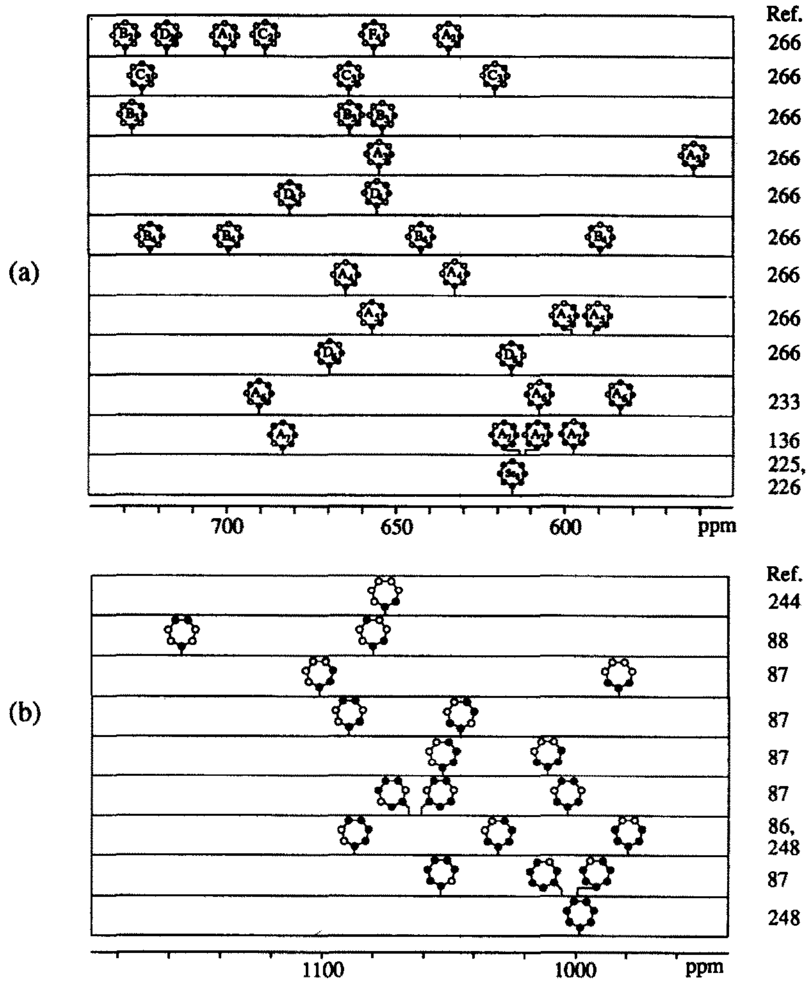

Fig. 9. Trends in the ^{77}Se chemical shifts in (a) Se_nS_{8-n} and (b) Se_nS_{7-n}.

tive trend within each of the three groups. When there are selenium atoms in positions 3–7 with respect to the active nucleus, the resonance is shifted downfield. These trends explain, for instance, why the chemical shift of Se_8 has the largest value of all the molecules with two selenium neighbors and the middle selenium atom of 1,2,3-Se_3S_5 shows the smallest chemical shift.

Independent verification on the above-described spectral interpretation can be obtained from the ^{77}Se NMR spectra of 1,2,3-Se_3S_5, 1,2,5,6-Se_4S_4 and Se_8 that can be prepared pure enough for the unambiguous assignment of NMR resonances. Natural-abundance 1,2,3-Se_3S_5 [226] exhibits two signals at intensity ratio of 2:1 at 654.2 and 560.6 ppm and 1,2,5,6-Se_4S_4 [89] and Se_8 [225] show resonances at 651.5 ppm and

614.6 ppm, respectively, as expected from the scheme deduced for the selenium sulfide mixtures.

The ^1J(SeSe) and ^2J(SeSe) coupling constants of the Se_nS_{8-n} species [226,233] lie in the range of 4.7–44.3 Hz reported for organic polyselenides [234]. The spectral analysis of $\mathbf{A_4}$, $\mathbf{B_4}$, $\mathbf{D_4}$, $\mathbf{A_5}$ and $\mathbf{A_6}$ [226,233] shows that the one-bond coupling is of a different sign from those of ^2J(SeSe) and ^3J(SeSe) coupling constants. Presumably this is also the case for $\mathbf{A_3}$, $\mathbf{B_3}$ and $\mathbf{C_3}$, but it cannot be deduced from the coupling patterns of these simple three-spin systems. The coupling constants of different selenium sulfide rings are compared in Table 7. Like the chemical shift, the ^1J(SeSe) coupling constants show a trend depending on the chemical environment of the Se–Se bond. In the case of the isolated bond (the structural unit –S–Se–Se–S–), the coupling is ca. 50 Hz. The end bond of a longer selenium fragment (the structural unit –S–Se–Se–Se–) shows a coupling of ca. 37 Hz and the bond surrounded by Se–Se bonds (the structural unit –Se–Se–Se–Se–) shows a still lower coupling of ca. 20 Hz.

It is interesting to note that two-bond coupling is more pronounced than one-bond coupling. Eggert et al. [234] have suggested that the magnitude of the coupling constants depends on the extent of interaction between the p lone-pair orbitals of the selenium atoms in question, as has been shown schematically in Fig. 10. The dihedral angles in the eight-membered chalcogen rings are close to 90° [47,51,55,81,89,94,98–104,133–136]. The overlap of the lone-pair p orbitals (and thus the coupling) between the adjacent selenium atoms is therefore minimized. With atoms i and $i+2$, the corresponding p lone-pairs are directed to the same region in space and have therefore a possibility to transfer coupling information.

^{125}Te and ^{77}Se NMR spectroscopy have recently been applied to study the molecular composition of sulfur-tellurium and sulfur-selenium-tellurium melts at 145°C [50]. The spectral assignment and the identification of the molecular species have again been made on the basis of combined information from the natural-abundance and from the ^{77}Se- and ^{125}Te-enriched samples (enrichment in both cases 92%) also taking into account the observed linear relationship between the ^{125}Te and ^{77}Se chemical shifts [$\delta(\mathrm{Te}) \approx 1.8\delta(\mathrm{Se})$] [235] in analogous compounds.

The melts were found to contain cyclic chalcogen molecules in equilibrium with polymeric material. The main tellurium-containing chalcogen ring in the binary sulfur-tellurium melt (Te content 1.5–10.0 mol%) was TeS_7 [$\delta(\mathrm{Te}) = 1316$ ppm]. The presence of small amounts of 1,2-Te_2S_6 [$\delta(\mathrm{Te}) = 1126$ ppm] and its other isomers was also inferred from spectroscopic data [50].

The ^{125}Te NMR spectrum of the ternary sulfur-selenium-tellurium melt containing 1.5 mol% of both ^{77}Se-enriched selenium and ^{125}Te-enriched tellurium is shown in Fig. 11. The melt was found to contain binary heterocycles SeS_7, all isomers of Se_2S_6, TeS_7 and 1,2-Te_2S_6 as well as its other isomers. The presence of ternary 1,2-$TeSeS_6$ [$\delta(\mathrm{Te}) = 1148$ ppm; $\delta(\mathrm{Se}) = 493$ ppm; $^1J(\mathrm{TeSe}) = 50$ Hz] and 1,3-$TeSeS_6$ [$\delta(\mathrm{Te}) = 1364$ ppm, $^2J(\mathrm{TeSe}) = 220$ Hz] as well as its 1,4- and 1,5-isomers can also be inferred from the spectrum in Fig. 11. The ^{77}Se and ^{125}Te NMR signals of the polymeric material could be

TABLE 7

^{77}Se–^{77}Se coupling constants of heterocyclic selenium sulfides

Molecule	Chemical shift	Intensity ratio	^{1}J(SeSe)	^{2}J(SeSe)	^{3}J(SeSe)	^{4}J(SeSe)	Ref.
1,2,3-Se_3S_5	654.2, 560.6	2:1	34[a]				226
1,2,4-Se_3S_5	727.4, 662.9, 653.0	1:1:1	54[a]	98	6		226
1,2,5-Se_3S_5	723.7, 662.9, 619.7	1:1:1	51[a]		12	19	226
1,2,3,4-Se_4S_4	664.4, 581.6	1:1	−39, −17	112	3		226
1,2,3,5-Se_4S_4	722.4, 669.0, 641.6, 588.9	1:1:1:1	−37, −35	114, 96	8	16	226
1,2,4,5-Se_4S_4	680.8, 655.4	1:1	−56	97	10	−0.5	226
1,2,3,4,5-Se_5S_3	657.9, 598.2, 591.2	2:1:2	−40, −23	110,108	5	−3	226
1,2,3,4,5,6-Se_6S_2	695.1, 607.8, 584.8	1:1:1	−46, −29, −23	107,105	7,6,15	−5	233
1,2,3,4,5-Se_5S_2	1087.1,1025.0, 978.9	2:1:1	−65, −47	95, 59	10	0	86
1,2,3,4-Se_4S_4	764.2, 651.2	1:1	−73, 0	115	0		233

[a] The absolute sign of the coupling constant is ambiguous.

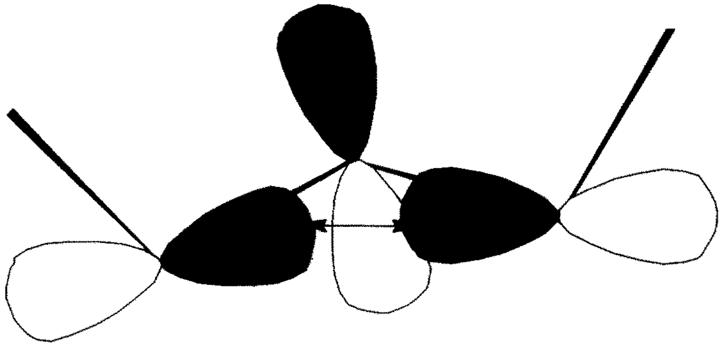

Fig. 10. The orientation of the p lone-pair orbitals in three adjacent chalcogen atoms. Eggert et al. [234] have used these spatial relationships to explain the relative magnitudes of ^{1}J(SeSe) and ^{2}J(SeSe) coupling constants.

interpreted in terms of the statistical distribution of the different $-E_1-E_2-E_3-$ fragments (E_1, E_2, E_3 = S, Se, Te) [50].

The mass spectrometric [49,236] and the Mössbauer [237] spectroscopic data also indicate the existence of TeS_7 in the sulfur-tellurium phases formed in the melt.

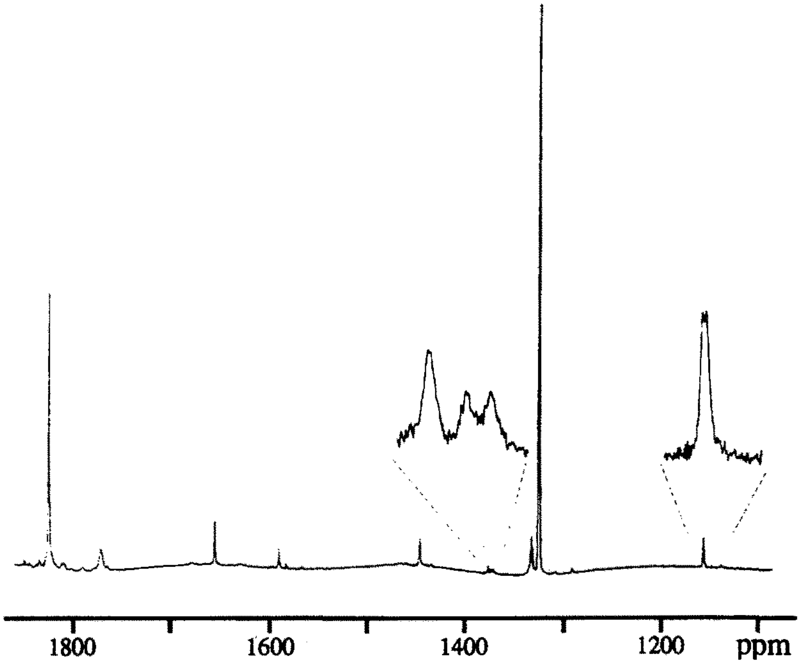

Fig. 11. ^{125}Te NMR spectrum of the ternary sulfur-selenium-tellurium melt containing 1.5 mol% of both ^{77}Se-enriched selenium and ^{125}Te-enriched tellurium (enrichment in both cases 92%). The spectrum has been recorded at 145°C [50] (© American Chemical Society).

E. SEVEN-ATOMIC RING MOLECULES

The seven-atomic chalcogen rings form an interesting class of compounds. The crystal structures have been determined for two different polymorphs of S_7 [129,130], 1,2,3,4,5-Se_5S_2 [85] and Te_nSe_{7-n} [52]. In solid state, all these molecules are found in the chair conformation. The crystal structure of Se_7 is unknown, but comparison of its vibrational spectrum [41] to the Raman spectra of the α-δ S_7 [238] indicates that it also has a similar structure to the other seven-atomic chalcogen rings. This is consistent with the existing X-ray data which show that the crystalline phase is orthorhombic and has 28 selenium atoms in the unit cell [40]. Further support is found in two ionic products $[Na(12\text{-Crown-}4)_2^+]_2Se_8^{2-}\cdot(Se_6,Se_7)$ [131] and $(NEt_4^+)_2[Se_5^{2-}\cdot 1/2Se_6\cdot Se_7]$ [132] which both contain a molecular Se_7 ring with a conformation similar to that in S_7 [129,130].

All seven-membered chalcogen rings contain a nearly coplanar fragment of four atoms (see Table 4) resulting in the significant alternation of the bond lengths throughout the molecule. This alternation has been explained by Steudel and Schuster [238] in terms of the mutual p lone-pair repulsion of the two central atoms in the planar four-atomic fragment and of the hyperconjugational interaction between these same lone-pairs and the empty σ^* orbitals of the bonds connecting the fragment to the rest of the molecule. These interactions are shown schematically in Fig. 12.

The molecular conformation of S_7 has been calculated using molecular mechanics [153], semi-empirical [168,173,239] and ab initio [186–189,241], as well as density functional [152] techniques. CNDO [240] has been used to interpret the photoelectron spectrum of orthorhombic selenium, and the density functional approach has also been applied for Se_7 [218] and 1,2-Se_2S_5 [242]. With the exception of the molecular mechanics calculations for S_7 [153] and the CNDO study of Se_7 [240], all techniques predict that the

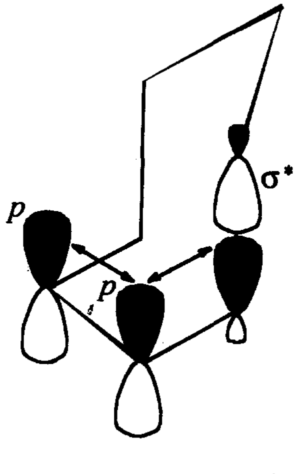

Fig. 12. Lone-pair interactions and hyperconjugation in the seven-membered chalcogen ring as suggested by Steudel and Schuster [238].

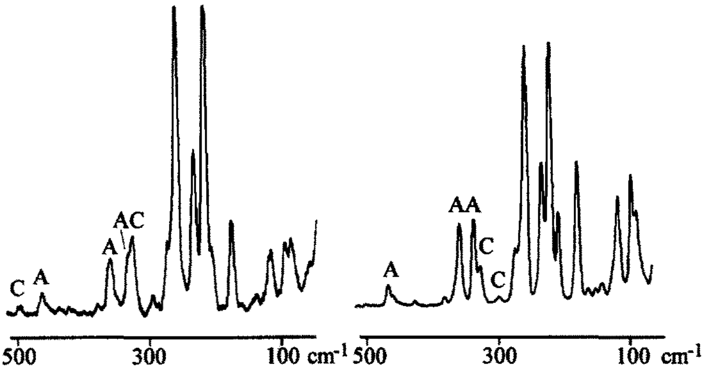

Fig. 13. The low-temperature Raman spectra of 1,2,3,4,5-Se_5S_2. Left: sample recrystallized from CS_2 at −50°C. Right: spectrum of the same sample after warming above −10°C [85] (© Angewandte Chemie).

ground-state has the chair-conformation with one torsional angle of ca. 0°. Dixon and Wassermann [187] and Raghavachari et al. [188,189] have noted that at (12s8p1d)/[5s3p1d] and HF/3-21G* levels of theory (respectively) the ideal C_s structure of S_7 has a very low imaginary frequency (21i and 18i cm^{-1}, respectively) indicating that the ideal C_s structure is not an energy minimum. By allowing a distortion to C_1 symmetry, a local minimum only 0.08 kJ mol^{-1} [187] or 0.8 kJ mol^{-1} [188,189] lower in energy was obtained. The inclusion of electron correlation, however, reversed the relative ordering of the two structures with C_s structure being more stable at all correlated levels. Therefore, the reliability of Hartree–Fock theory was questioned and the C_s form was taken as the more likely candidate for the ground-state of S_7 [188,189]. According to the density functional calculations of Hohl et al. [152], however, the distortion of the S_7 molecule from C_s symmetry costs practically no energy. The same is also true in the case of Se_2S_5 [242]. The unique torsional angle deviates slightly from 0° even in isomers where an idealized symmetry of C_s would be expected. It seems that the observed distortions of the seven-membered chalcogen rings are real intramolecular effects and not caused by packing in the solid state.

Urey–Bradley force field calculations have been utilized in the assignment of the vibrational spectra of S_7 [238], and 1,2-Se_2S_5 [82,243] and 1,2,3,4,5-Se_5S_2 [85,243]. The power of the vibrational analysis is exemplified by the assignment of the two low-temperature Raman spectra of 1,2,3,4,5-Se_5S_2 which are shown in Fig. 13. The calculated fundamental vibrations for the different isomers of the molecule are illustrated in Fig. 14. Only isomers in the chair conformations have been included, since that is the observed conformation of the molecule in the solid state [85]. It can be clearly seen that the stretching vibrations are sensitive probes for the presence of a particular isomer in the solid state. Comparing the calculated and observed wavenumbers it was concluded that the solid lattice consisted of two isomers labelled **A** and **C** (see Fig. 14). The relative content of the isomer **A** gets higher the higher the temperature of crystallization. At −78°C, the two isomers are present in the ratio of **A** to **C** of 1:1, whereas at room temperature it is

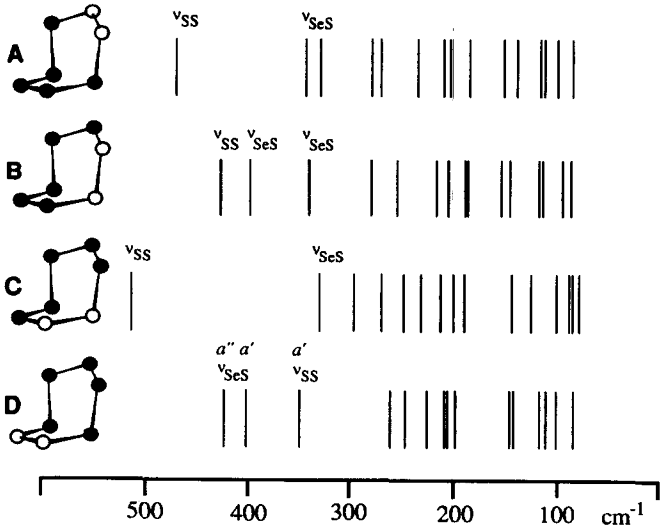

Fig. 14. Fundamental vibrations of the four isomers of 1,2,3,4,5-Se_5S_2 calculated using the Urey–Bradley force field [243].

4:1 [85]. The disorder scheme found during the crystal structure determination at room temperature confirms these conclusions.

The seven-membered chalcogen rings have also proved to be fluxional undergoing facile pseudorotation. This was first suggested by Steudel and Schuster from thermodynamic vapor phase data [238]. The pseudorotation is shown schematically in Fig. 15 and can best be described for S_7 (or Se_7) [Fig. 15(a)]. Consider the pseudorotation of 90° about the unique S–S bond (bond 7). The subsequent adjustment of all bond lengths to accommodate the changed chemical environments of all sulfur atoms creates a different, but identical S_7 molecule. An intermediate with C_2 symmetry is obtained upon pseudorotation of 45°. From this intermediate, another pathway can be conceived involving the pseudorotation about bond 1 that is unique in C_2 symmetry. This creates a molecule in boat conformation. The complete pseudorotation scheme of S_7 thus involves two series of identical molecules with a common intermediate.

The barriers of rotation about the S–S bond form a basis for discussing the energetics of the pseudorotation. There have been several ab initio calculations carried out on the rotational barriers using sulfanes as model compounds [120–122,245 and refs. therein] which indicate that the *cis*-barrier is 25–30 kJ mol^{-1} with the *trans*-barrier of the same order of magnitude or somewhat lower. The recent millimeter-wave and far-infrared spectral data on the internal rotor HSSH yields barrier heights of 33.5 and 23.8 kJ mol^{-1} for the *cis*- and *trans*-barriers, respectively [123]. It is also in agreement with the barriers obtained for acyclic disulfides using NMR spectroscopy [246]. It was estimated that the rotational barrier of the S–S bond in the absence of steric effects is ca. 28 kJ mol^{-1} with the *trans*-barrier probably higher than the *cis*-barrier.

Steudel [247] has suggested that the torsional strain of the S_7 molecule can be regarded as restricted to the unique S–S bond. Therefore, the enthalpy of formation of S_7 from the strainless S_8 (24 kJ mol^{-1}) can be thought to give an estimate for the torsional barrier. The relative energies of the different conformations of S_7 [152,173,188,189,241] and Se_2S_5 [242] calculated at various levels of theory also provide means to estimate the barriers of pseudorotation. The original estimate of Steudel [247] is well reproduced by these calculations. The low imaginary torsional frequency calculated for S_7 [187–189] and the energetically favorable distortion from the C_s symmetry [152] also indicate a facile pseudorotation as does (indirectly) the CNDO result which predicts the twist (C_2) conformation of Se_7 to be energetically slightly more favorable than the chair (C_s) conformation [240].

There is also experimental evidence to support the concept of pseudorotation in the seven-atomic chalcogen rings. The Raman spectrum of S_7 in solution [244] produces significantly broader bands than observed for a sample in the solid state [238]. ^{77}Se NMR spectroscopy also provides convincing experimental evidence on the pseudorotation. For instance, Se_7 shows a single resonance at 996 ppm [248] even though four signals at the

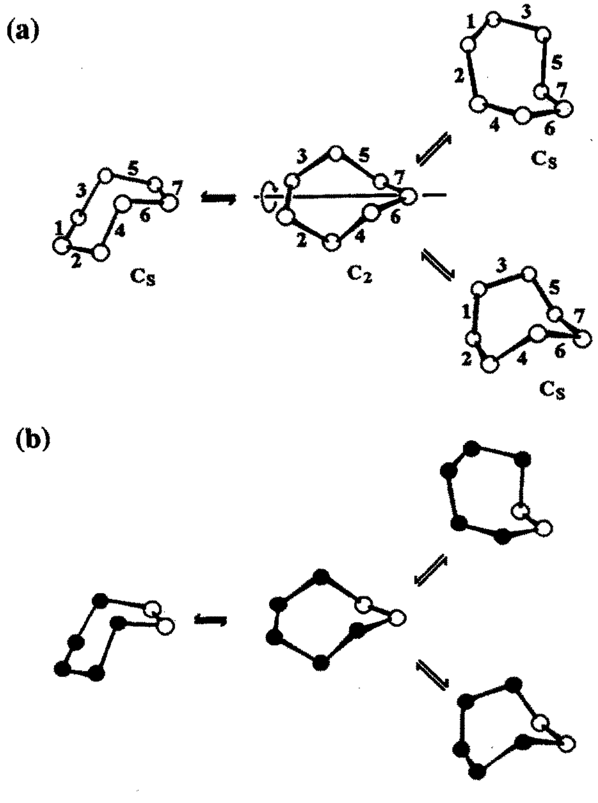

Fig. 15. The pseudorotation scheme in (a) S_7 and (b) 1,2,3,4,5-Se_5S_2 [86] (© American Chemical Society).

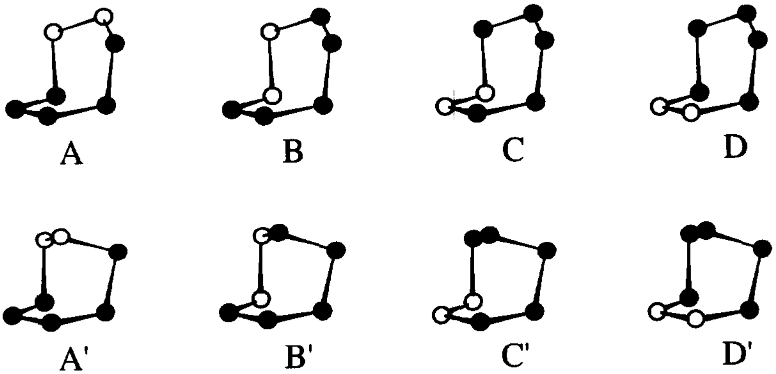

Fig. 16. The different possible isomers of 1,2,3,4,5-Se$_5$S$_2$ in chair and boat conformations [86] (© American Chemical Society).

intensity ratio of 1:2:2:2 would be expected according to the solid state molecular geometry (see Table 4). In the following, the ^{77}Se NMR spectroscopic evidence on the pseudorotation of 1,2,3,4,5-Se$_5$S$_2$ is described in more detail.

The pseudorotation of 1,2,3,4,5-Se$_5$S$_2$ is shown in Fig. 15(b). It is analogous to that in S$_7$ but does not produce identical molecules. It can be seen from Fig. 15(b) that the S–S bond can wander around the seven-membered heterocycle producing eight different isomers with a molecular symmetry of C_s of which four are found in the chair conformation and four in the boat conformation. The eight isomers are shown in Fig. 16. In addition, there are also four isomers with C_2 molecular symmetry. Optical isomers are not included in the discussion, since they cannot be distinguished by NMR.

The ^{77}Se NMR spectrum of 1,2,3,4,5-Se$_5$S$_2$ shows three signals at 1087.1, 1025.0 and 978.9 ppm with an intensity ratio 2:1:2 [86,248]. In the spectrum of the ^{77}Se-enriched sample, all these resonances appear as complicated second-order multiplets [86] (see Fig. 17). The spectrum was simulated as a five-spin [AMM'XX'] system with an excellent fit between the observed and calculated transitions. The coupling constants of 1,2,3,4,5-Se$_5$S$_2$ are shown in Table 7.

It can be seen from Fig. 16 that if the molecule undergoes no pseudorotation, only the isomers **D** and **D'** are consistent with the spectral information, since all other isomers should show five signals in the NMR spectrum. Comparison of the trends in the observed coupling constants with those found in the calculated reduced coupling constants [86] strongly indicate that all possible isomers of 1,2,3,4,5-Se$_5$S$_2$ in chair-, boat- and twist-conformations (C_2) co-exist and rapidly interconvert in solution. It has been discussed above that, in the solid state, the molecule shows a chair conformation with isomers **A** and **C** predominant in the lattice [85]. It is unlikely that in solution the molecule would assume a discrete isomeric form different from those in the solid state.

Similarly, only one resonance at 1077.3 ppm is observed for 1,2-Se$_2$S$_5$ [244] which either indicates an isomer with the selenium atoms occupying the two central atom posi-

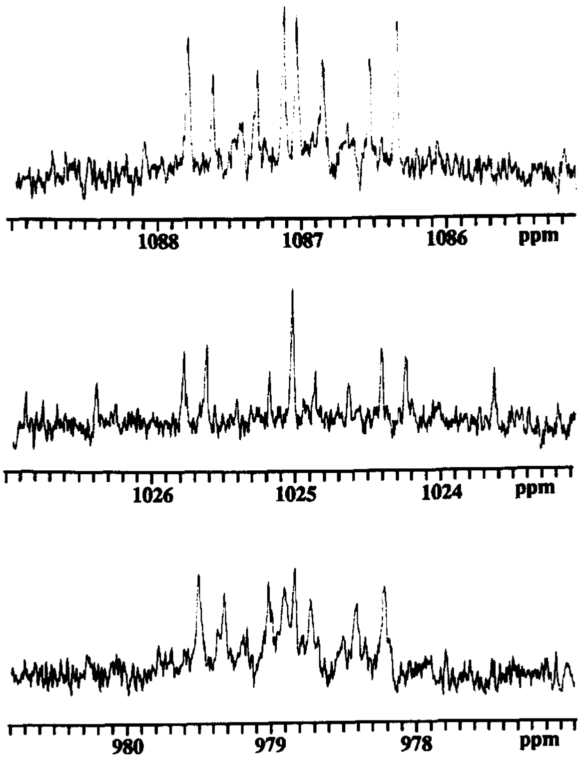

Fig. 17. ^{77}Se NMR spectrum of 1,2,3,4,5-Se_5S_2 containing ^{77}Se-enriched selenium (enrichment 92%) [86] (© American Chemical Society).

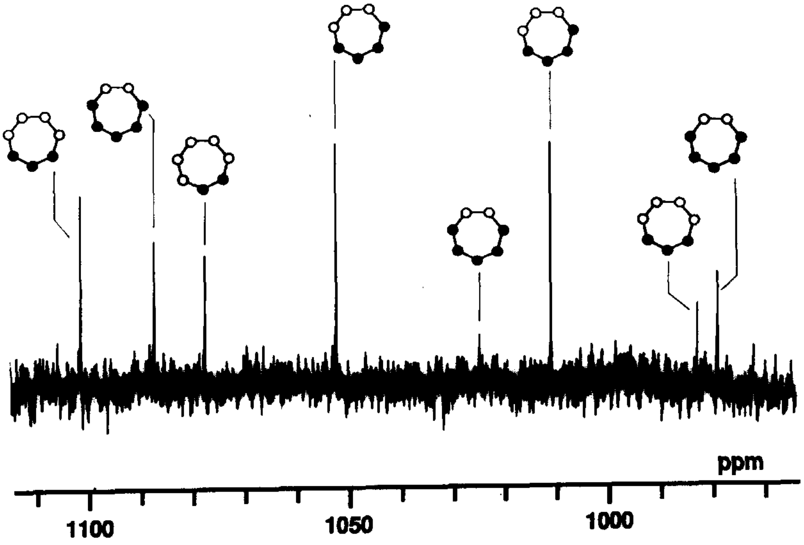

Fig. 18. ^{77}Se NMR spectrum of Se_nS_{7-n} species prepared by the reaction of $[Ti(C_5H_5)_2Se_nS_{5-n}]$ with S_2Cl_2 [87] (© Royal Society of Chemistry).

TABLE 8

The product distribution (in mol%) of heterocyclic Se_nS_{7-n} molecules prepared from $[Ti(C_5H_5)_2Se_nS_{5-n}]$ [87]

$[TiCp_2Se_nS_{5-n}]$[a]	S_2Cl_2			Se_2Cl_2		
	Product	Pred.	Obs.	Product	Pred.	Obs.
$[TiCp_2Se_5]$ (30%)	1,2,3,4,5-Se_5S_2	30	21	Se_7	30	34
$[TiCp_2Se_4S]$ (32%)	1,2,3,4-Se_4S_3	32	33	1,2,3,4,5,6-Se_6S	32	22
$[TiCp_2Se_3S_2]$ (10%)	1,2,3-Se_3S_4	10	27	1,2,3,4,5-Se_5S_2	10	10
$[TiCp_2SSe_3S]$ (17%)	1,2,3-Se_3S_4	17		1,2,3,5,6-Se_5S_2	17	18
$[TiCP_2SSe_2S_2]$ (11%)	1,2-Se_2S_5	11	18	1,2,4,5-Se_4S_3	11	17

[a] The content of the selenium-containing $[Ti(C_5H_5)_2Se_xS_{5-x}]$ in the starting material has been determined with ^{77}Se NMR spectroscopy [249].

tions in the coplanar fragment of four atoms or necessitates rapid pseudorotation. On the basis of the arguments described above, the former alternative can be ruled out.

It has recently been shown that bis(cyclopentadienyl)titanium selenide sulfide mixtures $[Ti(C_5H_5)_2Se_nS_{5-n}]$ can be prepared by reacting $[Ti(C_5H_5)_2Cl_2]$ with an approximately equimolar mixture of lithium polysulfides and polyselenides [249]. These mixtures were characterized by X-ray crystallography and ^{77}Se NMR spectroscopy. By treating $[Ti(C_5H_5)_2Se_nS_{5-n}]$ with S_2Cl_2 or Se_2Cl_2, a number of seven-membered selenium sulfides can be prepared [87]. They were identified by using ^{77}Se NMR as exemplified in Fig. 18 for the reaction of $[Ti(C_5H_5)_2Se_nS_{5-n}]$ and S_2Cl_2. It is easy to see that the trends in chemical shifts in the seven-atomic rings are analogous to those in eight-atomic rings describe above (see Fig. 9(b)). Comparison of the predicted product distribution of the Se_nS_{7-n} molecules from the known composition of the starting $[Ti(C_5H_5)_2Se_nS_{5-n}]$ mixture with that determined semiquantitatively from the peak intensities is shown in Table 8 and supports the spectral assignment.

F. SIX-ATOMIC RING MOLECULES

There are three six-membered chalcogen ring molecules with known crystal structures, namely S_6 [126,127], Se_6 [128] and Se_5S [85]. The cyclohexasulfur molecule is also found in the addition compound $S_6 \cdot S_{10}$ [77,78] and Se_6 in the two ionic products $[Na(12\text{-crown-}4)_2{}^+]_2Se_8{}^{2-} \cdot (Se_6,Se_7)$ [131] and $(NEt_4{}^+)_2[Se_5{}^{2-} \cdot 1/2Se_6 \cdot Se_7]$ [132]. In all cases, the molecule is hexagonal and assumes the chair conformation (see Table 4). The crystal structure of Se_5S is disordered as expected [85] and the molecule shows an apparent site symmetry of D_{3d} like S_6 [126,127] and Se_6 [128]. The six-membered ring in $S_6 \cdot S_{10}$ has a site symmetry of C_i [78], but the bond parameters are very close to those in free S_6. The Se_6 rings found in the two polyselenides [131,132] are somewhat more distorted.

Vibrational spectra of S_6 [3–6,77,78,250–253] and Se_6 [8,9,254,255] are well known and have been assigned with normal coordinate analysis using the modified Urey–Bradley force field [251,254,255]. The same force field was utilized in the calculation of fundamental vibrations of eleven possible selenium sulfide ring molecules Se_nS_{6-n}. The force constants were adapted from S_6 and Se_6. While it is not easy to identify individual molecular species from a complicated mixture by use of vibrational analysis, it was possible to assign the Raman spectrum of SeS_5 that can be prepared stoichiometrically pure [243].

The ab initio MO calculations of vibrational frequencies have traditionally been problematic. Good agreement between the experimental and calculated wavenumbers requires good quality basis sets. The frequencies of S_6 have been calculated at various levels of theory [187–189,256] and are shown in Table 9 together with observed fundamental vibrations. Dixon and Wasserman [187] note that while the overall agreement between the calculated and observed wavenumbers is fair, there are certain discrepancies. For instance, the a_{1u} mode that is forbidden both in IR and Raman spectra has been assigned the experimental value of 390 cm^{-1} [250,251]. The calculated value of Dixon and Wasserman [187] of 466 cm^{-1} is clearly too large. Raghavachari et al. [188,189] cite a somewhat closer agreement. A reasonable agreement is only obtained when going beyond Hartree–Fock theory [256].

Whereas seven-membered chalcogen rings are fluxional, six-membered rings seem to be rigid. As shown in Table 4, all known molecules assume the chair conformation (D_{3d}). When using the polarized basis set, the equilibrium geometry of S_6 calculated with ab initio techniques [187–189,241,256] is in good agreement with the observed ground-

TABLE 9

Calculated and observed vibrational frequencies of S_6

Mode	HF/DZP[a]	HF/3-21G*	MP2/DZP[b]	Experimental	
	[187]	[188,189]	[256]	Raman [77,78]	IR [250,251]
a_{1g}	475	457	493	471(100)	
e_u	468	447	472	462(2)	463 s
e_g	482	457	462	451(44)	
a_{1u}	466	439	399		390 vw
a_{2u}	324	325	323		313 s
a_{1g}	259	259	270	266(55)	
e_g	213	214	209	203(86)	
e_u	159	159	166		180 s
Lattice				106(3)	
vibrations				84(46)	

[a] (12s8p1d)/[5s3p1d] basis.
[b] (11s7p1d)/[6s4p1d] basis.

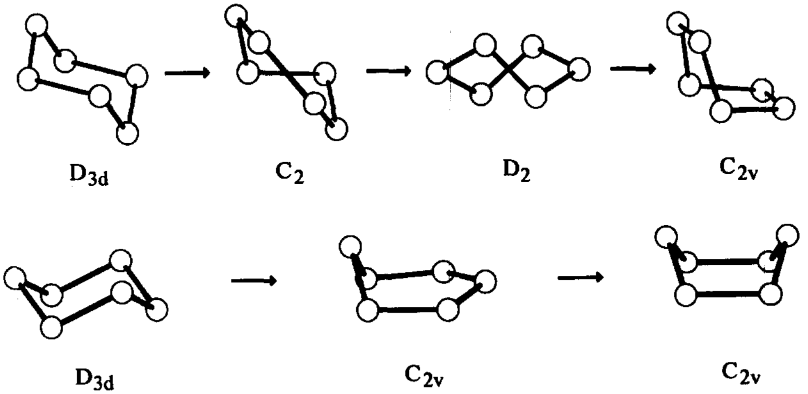

Fig. 19. Two possible routes for the inversion of the six-membered ring molecule from the chair conformation to the boat conformation.

state molecular structure [126,127]. When the basis set is not augmented by polarization functions, the bond is estimated to be too long as expected [186,256]. The density functional approach for S_6 [152] and Se_6 [218] also reproduces the experimental geometry, but semi-empirical methods [168,170,173] all predict shorter bonds.

According to ab initio results, the boat conformation of S_6 (C_{2v}) lies 50–70 kJ mol^{-1} above the chair conformation depending on the level of theory [153,188,189,241]. The density functional approach [152], molecular mechanics, [153] and SINDO1 calculations [239] yield energetics in good agreement with the ab initio values, but parametrized molecular dynamics [196,197], MNDO [168,173] and CNDO [257] predict much smaller energy differences between the chair and boat conformations. Hohl et al. [218] note for Se_6 that there is a low-lying local minimum for the boat conformation, but do not give its relative energy.

The inversion to the boat conformation can be thought to proceed by two routes: by direct inversion or by pseudorotation about any bond of the molecule. These two routes are illustrated in Fig. 19. Direct inversion involves a semi-planar conformation (C_s) as an intermediate. Ab initio calculations predict this conformation to be a transition state and lie 128–137 kJ mol^{-1} above the chair conformation [188,189,241]. CNDO results [257] place it at 95.6 kJ mol^{-1} and MNDO calculations [168] only 61.5 kJ mol^{-1} above the ground-state.

The pseudorotation about any of the six bonds of S_6 proceeds through two twist conformations as shown in Fig. 19. The MP2/3-21G* calculations [241] show that the C_2 twist lies 131.6 kJ mol^{-1} above the chair conformation and represents the energy barrier for this pathway. Upon continued pseudorotation, the D_2 twist conformation is formed. This conformation represents a local minimum and lies 57.4 kJ mol^{-1} above the chair conformation [241]. The boat conformation is easily reached from the D_2 twist and has MP2/3-21G* energy of 63.3 kJ mol^{-1} relative to the ground-state.

The other ab initio calculations [153,188,189] place the D_2 twist and the boat conformation (C_{2v}) at 52.7–60.1 kJ mol^{-1} and 58.7–66.5 kJ mol^{-1}, respectively, above the ground-state with the boat conformation always above the D_2 twist. Electron correlation has only a minor effect on the energy. The molecular mechanics calculations are also in agreement with these results [153,258].

Since both pathways for the inversion of S_6 shown in Fig. 19 have very high barriers, the interconversion from the chair conformation to the boat conformation or vice versa must be considered unlikely. The MO results indicate, however, that the boat conformation, once formed, should be relatively stable against inversion to the chair conformation. Although there is no information for the neutral chalcogen rings in the boat conformation, there are some speculations on its properties [257]. A cationic $Te_nS_{6-n}^{2+}$ is known to exist in the boat conformation [259]. The SCF-Xα-SW calculations of Salahub et al. [180] also predict a boat conformation for valence isoelectronic S_6^{2+}.

It is interesting to note that the boat conformation does not represent a local minimum, but rather a transition state between two D_2 twist conformations [188,189,241]. The small energy difference of 3–6 kJ mol^{-1} [188,189,241] between the two conformations implies that the D_2 twist is fluxional, undergoing facile pseudorotation in solution at ambient temperatures like the seven-membered chalcogen rings.

The ^{77}Se NMR spectral properties of Se_nS_{6-n} molecules are much less established than those for Se_nS_{8-n} and Se_nS_{7-n} species. The identification of the unknown molecular species is more problematic for the six-membered ring molecules than for the eight- or seven-membered molecules, because of all the thirteen possible Se_nS_{6-n} ($n = 0$–6) species (see Fig. 20), one is not observable in ^{77}Se NMR and seven show only singlets even when ^{77}Se-enriched selenium is used in the preparation of the samples.

The ^{77}Se chemical shifts have been reported for SeS_5 [244], 1,2,3,4-Se_4S_2 [233],

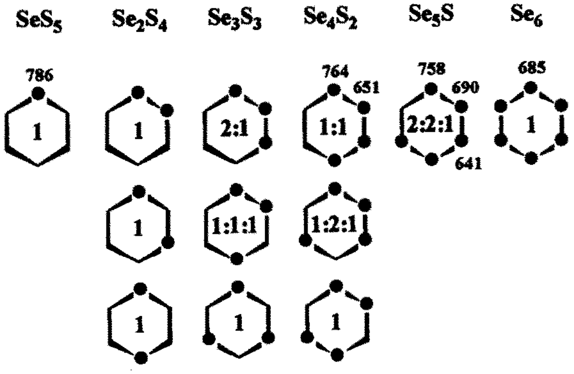

Fig. 20. The different Se_nS_{6-n} ring molecules. The known ^{77}Se chemical shifts are indicated for individual atoms in different molecules: SeS_5 [244], 1,2,3,4-Se_4S_2 [233], Se_5S [136] and Se_6 [225].

SeS_5 [136] and Se_6 [225] and are indicated in Fig. 20. Because 1,2,3,4-Se_4S_2 has been studied using ^{77}Se-enriched selenium [233], its ^{77}Se–^{77}Se coupling constants are also known (see Table 7). From these data and from the trends deduced from the eight-membered selenium sulfide heterocycles [226], it is possible to make some inferences on the appearance of the yet unobserved singlets.

The resonances due to 1,3-Se_2S_4, 1,4-Se_2S_4 and 1,3,5-Se_3S_3 should appear near to 786 ppm observed for SeS_5 [244], possibly slightly downfield. The signals of 1,2-Se_2S_4 and 1,2,4,5-Se_4S_2 come from selenium atoms with one selenium and one sulfur neighbor and therefore should appear upfield from the resonance of SeS_5. The end atom of the –Se_4– fragment in 1,2,3,4-Se_4S_2 and that of the –Se_5– fragment in Se_5S both have one selenium and one sulfur neighbor and show a resonance at 764 [233] and 758 ppm [136], respectively. Therefore, this is the region where the resonances of 1,2-Se_2S_4 and 1,2,4,5-Se_4S_2 are expected. All other Se_nS_{6-n} molecules have both chemically and magnetically inequivalent selenium nuclei. The assignment of chemical shifts can be based on their constant expected intensity ratios, on their dependence on the environment, and, if ^{77}Se-enriched selenium is available, on the coupling patterns.

Takahashi et al. [260] have recorded the X-ray photoelectron spectrum of Se_6 and interpreted it with help of CNDO/S calculations.

G. MOLECULES OF OTHER RING SIZES

(i) E_3–E_5

The ground-state geometries of small chalcogen molecules have been under debate during recent years. Although small sulfur and selenium species have been observed in the vapor, there is very little experimental evidence on their structures. There is, however, an abundance of theoretical studies that contribute to the understanding of these systems.

The three-membered chalcogen molecules can be thought to have an open chain structure (C_{2v}) like O_3 and SO_2, or a ring structure (D_{3h}). All single-configuration HF calculations of S_3 [189,261–269] predict the ring to be more stable than the open chain form regardless of the level of theory. When electron correlation is taken into account, the order of stability is reversed. A detailed study of Rice et al. [264] demonstrates the effect of different levels of electron correlation on the relative energies of open chain and ring forms of S_3. The two minima were concluded to be close to each other in energy and thus both isomers should be observable.

This near degeneracy of the open chain and ring structures of S_3 was also found by the density functional [270,271] and molecular dynamics calculations [152,196] with the open form somewhat lower in energy. The semi-empirical methods [168,173,239,272] and the discrete variational Xα method (DVM-Xα) [273] predict the cyclic isomer to be the ground-state, even though the examination of Xα-SW orbital energies and wave functions [180] led to a conclusion that an open form with a bond angle of ca. 120° is a reasonable ground-state. When coupling the DVM-Xα method with the transition state approach to the binding energy [274], the open chain ground state is found to be lower in energy.

Basch [269] and von Niessen et al. [275] have extended the argument of the geometry of E_3 molecules to selenium and tellurium. It was concluded that the open chain and cyclic isomers of both Se_3 and Te_3 should have nearly the same total energy. Basch [269] concluded that the stability of the ring isomer increases when moving down the chalcogen group. Simultaneously, the barrier to the interconversion between the two isomers is lowered. The MD DF study of Hohl et al. [218] for Se_3 is in agreement with these conclusions.

S_3 has been reported to show a visible absorption at $\lambda_{max} = 410$ nm [156,276, 277,278], an ionization energy of 9.68–10.2 eV [279,280], and an electron affinity of 2.093(25) eV [281]. Von Niessen and Tomasello [266] have used the Green's function method to interpret the ionization energy and electron affinity data of S_3 in terms of the open chain structures and von Niessen et al. [275] have extended the treatment to Se_3 and Te_3. The resonance Raman spectrum of S_3 [282,283] as well as that of the matrix isolated Se_3 [284] have been assigned in terms of the open chain structures. The IR spectrum of isotopically enriched S_3 in solid argon [285] also indicates an open (C_{2v}) structure.

The ground state geometry of S_4 is subject to even more confusion than that of S_3. Because the appearance potential of S_4 was found to be higher than that of S_6, S_7 and S_8, it was thought possible that the most stable isomer is not a ring [280]. There is also a multitude of theoretical studies of the molecule some of which have dealt with the ground-state geometry and advocate different candidates from among the possible isomers shown in Fig. 21 [152,153,155,156,167,168,170,171,173,180,187,189,196,197,218, 239,262,284,286–291]. The most sophisticated theoretical treatment to date is that of Quelch et al. [289] who also give a comprehensive review of the problem. Their ab initio study includes basis sets of double and triple zeta quality with polarization functions and considers the effects of electron correlation at different levels of theory. The global minimum of S_4 is predicted to be a singlet *cis*-planar chain of C_{2v} symmetry with several low-lying states the closest being the *trans*-chain (ca. 40 kJ mol^{-1} above the global minimum) and followed by almost degenerate triplet *trans*- and helical chains and then by a puckered ring and a branched three-membered ring that are also almost degenerate. The assignment of the fundamental vibrations [213,292] and of the electronic absorptions [276–278,293] in terms of *cis*- and *trans*-chains of S_4 is also discussed by Quelch et al. [289]. It is worth noting that there is no ambiguity in the geometry of the four-atomic cation E_4^{2+}. A square planar ring is observed both experimentally and theoretically [13,291 and refs. therein].

Compared to S_3 and S_4, there seems to be better consensus that the five-membered chalcogen species form cyclic molecules. The ionization energies [279], appearance potentials [280] and the HPLC analysis carried out in connection with solution photolysis of sulfur molecules [294] indicate that S_5 is a ring molecule. This is supported by the evidence on the existence of $S_5{=}O$ with a five-membered sulfur ring [295]. All theoretical studies seem to agree that an envelope-shaped ring (C_s) is the most stable conformation

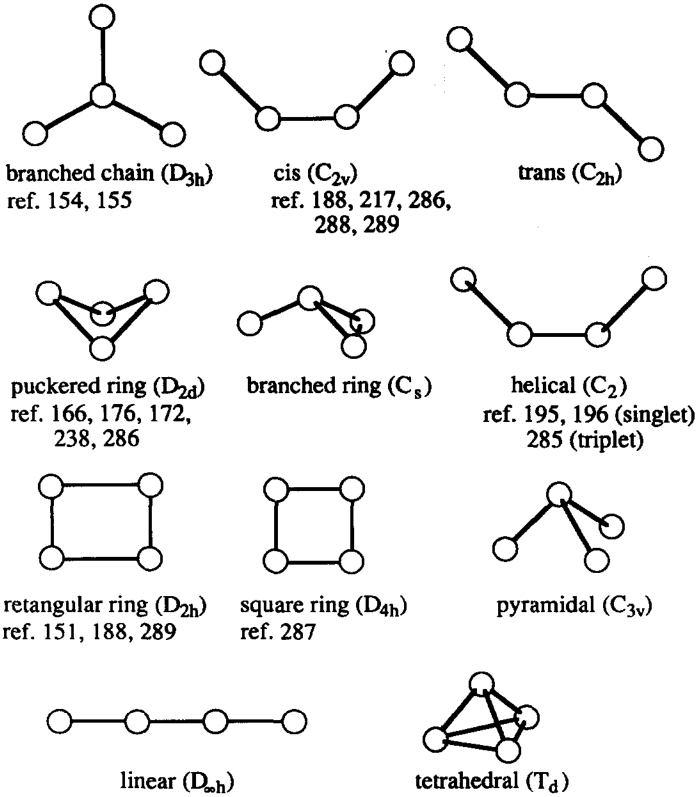

Fig. 21. Isomers of S_4. The suggestions for the ground-state have also been indicated.

for S_5 [152,153,168,173,187,189,239,296] and Se_5 [218]. The half-chair form (C_2), however, was found to be almost degenerate with the envelope, implying facile pseudorotation like that in seven-membered chalcogen rings (see above). It is interesting to note that the parametrized molecular dynamics calculations disagree with all above-listed theoretical studies and predict a planar five-membered ring [196,197].

(ii) E_9–E_{20}

The molecular structures of S_{10} [78,137], S_{11} [75,138], S_{12} [76,139], S_{13} [75], α-S_{18} [60,140] and β-S_{18} [141] and S_{20} [60,61] are shown in Table 4. The Raman spectra of S_{10} [77,78], S_{11} [74,75], S_{12} [253,297,298], S_{13} [74,75], α-S_{18} [33] and S_{20} [33] have also been reported. Two polymorphs of S_9 [105] and S_{15} [79] have also been identified using vibrational spectroscopy. In addition to an early molecular mechanics study [153], ab initio MO [188,189,299] MD DF [152] calculations have recently been performed for sulfur rings S_9–S_{13}. The optimized ground-state geometries of S_{10}–S_{13} with both techniques are in good agreement with the experiment. It has not been possible to obtain single crystals for S_9 and consequently no molecular structure is known. Steudel et al. [105], however, predict a C_2 symmetry for the molecule with bond lengths ranging from 203 to 209 pm and torsional angles from 70 to 130°. Thus, the molecule is not expected to have a planar four-atomic fragment like in S_7 or S_5. The geometries obtained both with ab initio [188,189] and MD DF [152] calculations are in perfect agreement with these estimates. Raghavachari et al. [188,189] have shown by frequency calculations that the C_2 is a true minimum on the potential energy surface. Hohl et al. [152] predict three low-lying structures none of which conform to the Raman spectroscopic data [105]. These structures are reported to lie ca. 20 kJ mol^{-1} above the ground-state [152]. All four structures of S_9 are shown in Fig. 22.

The only structurally characterized selenium sulfide of ring size larger than eight is a twelve-membered species containing a mixture of Se_nS_{12-n} and S_{12} [65]. It is isostructural with S_{12} [139]. Steudel et al. [83] report the formation of 1,2-Se_2S_{10} and 1,7-Se_2S_{10} as a result of dimerization of SeS_5 and discuss the Raman spectra of the products in terms of the possible structures derived from S_{12} [139] and $S_{12} \cdot CS_2$ [76].

H. OXYGEN RINGS

In the ground-state, ozone O_3 is known to have a singlet open chain (C_{2v}) structure. However, theoretical calculations predict a low-lying singlet ring (D_{3h}) ca. 100 kJ mol^{-1} above the ground state (see the surveys in [264,269,300]).

The theoretical work by Schaefer's group on cyclic O_4 [301], O_6 [256,302], O_8 [190], and O_{12} [299] was motivated by the idea that oxygen rings might be viable as high energy density materials. If these rings lie in the relative minima on their potential energy

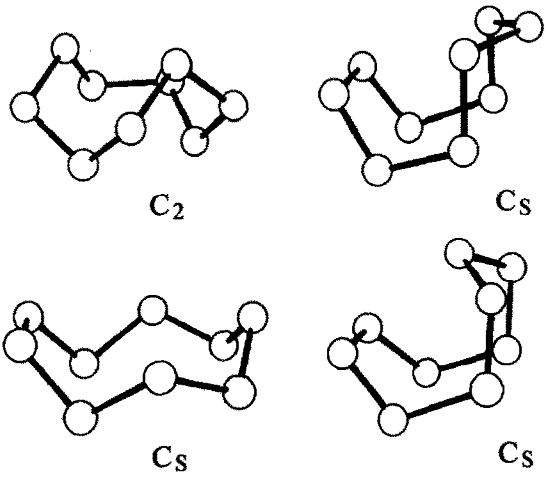

Fig. 22. Isomers of S_8 [152] (© American Institute of Physics).

surfaces, they could store a large amount of energy and be used to design improved fuels [190].

Calculations on O_4 have been performed by Feng and Novaro [263] and Seidl and Schaefer [301]. The latter report a DZP SCF CISD study for cyclic O_4. The molecule was predicted to be puckered (D_{2d}) with an O–O bond length of 139.2 pm and a torsional angle of 25°. The calculated frequencies showed the molecule to be a minimum on the energy surface. The planar ring was calculated to lie 12.1 kJ mol^{-1} above the puckered ring as a transition state. The calculated energy of decomposition of cyclic O_4 to two O_2 molecules at infinite distance was ca. 400 kJ mol^{-1}.

The structures and energetics of the larger oxygen rings have been studied with up to triple zeta plus double polarization basis set for O_6 [256,302] and with up to double zeta plus polarization basis set for O_8 [190] and O_{12} [299] all including the second-order Møller–Plesset perturbation theory for electron correlation. The geometries of all oxygen rings were similar to those of analogous sulfur molecules for which experimental information is available (cf. Table 4). Vibrational frequencies and IR and Raman intensities have been predicted for each molecule [190,256,299,302] and indicate an energy minimum, if a shallow one. Jones and Hohl [203], on the other hand, reported that while a density functional study of O_8 yields a geometry that is in good agreement with the DZP geometry of Kim et al. [190], the symmetric structure (D_{4d}) does not appear to be the most stable one. Rather, a ring with alternating bond lengths (C_{4v}) lies ca. 50 kJ mol^{-1} below the symmetric ring. After the optimization, the O–O bonds alternated between 143 and 150 pm [203].

The decomposition of oxygen ring into O_2 molecules is an exothermic process while that involving sulfur is endothermic. This has been qualitatively explained by Seidl and Schaefer [301] in terms of the weaker O–O single bond with respect to the S–S single bond and of the stronger O=O double bond with respect to S=S double bond. The "back-of-the-envelope" calculations of Seidl and Schaefer [301] suggest that unstrained O_n rings (i.e. $n \geq 6$) lie ca. 100 kJ mol^{-1} above $n/2$ isolated O_2 molecules. The results from ab initio calculations for O_4, O_6, O_8, and O_{12} are compared in Table 10. O_8 [190] and O_{12} [299]

TABLE 10

The energy of the decomposition reaction $O_n \rightarrow n/2\ O_2$ (in kJ mol^{-1} of oxygen atoms)

Basis set	O_4 [301]	O_6 [256]	O_8 [190]	O_{12} [299]
DZ SCF		95.4	89.1	87.4
DZP SCF	135.4	95.0	90.4	90.4
DZP MP2		70.3	64.4	
DZP CISD	118.4 109.8[a]			
TZ2P SCF		97.5		
TZ2P MP2		69.0		

[a] The CISD value after the application of the Davidson correction (see [301]).

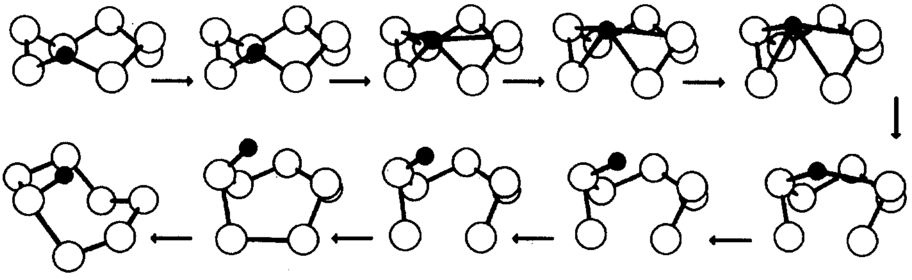

Fig. 23. Rearrangement pathway of S_7O [202,203].

seem to be more stable than anticipated by the qualitative estimates [301]. Kim et al. [190] suggest that the best opportunity for the detection of O_8 would be the observation of $\nu(b_2)$ band around 700 cm^{-1} during a matrix isolation IR experiment.

Hohl et al. [203,303] have introduced one oxygen into an eight-membered sulfur ring. It was shown by MD DF calculation: that a heterocyclic S_7O ring with a –S–O–S– has a local minimum in the energy surface. When kinetic energy corresponding to a temperature of 2000 K is applied, a rearrangement is triggered. The oxygen atom moves out of the ring and forms an exocyclic double bond to an S_7 ring. The process is shown in Fig. 23. Compounds with exocyclic sulfur–oxygen double bonds are also experimentally known. Their preparation, structures and properties have been reviewed by Steudel [4–6,9,20–22].

I. MOLECULAR COMPOSITION OF CYCLIC CHALCOGEN MIXTURES

It has been discussed in Section B that many preparative routes producing cyclic chalcogen molecules often form mixtures of several species (see Table 2). The facile interconversion reactions of the cyclic chalcogen molecules also result in the formation of mixtures of several species even when the starting material is stoichiometrically pure. The development of modern instrumental techniques of analysis has enabled rapid progress to be made in the identification and quantitative determination of discrete molecules even in complicated mixtures. Raman spectroscopy is a useful method for characterizing solid mixtures of homocyclic sulfur and selenium molecules. However, it is not possible to fully characterize the very complicated molecular system of heterocyclic selenium sulfides as discussed in Section D(iii). Reversed-phase HPLC can be used for the qualitative and quantitative analysis of chalcogen rings in organic solutions. The composition of liquid sulfur has also been determined by HPLC. The relative content of species containing selenium or tellurium can be conveniently analysed with NMR. Mass spectrometry has given information on the composition of sulfur, selenium, and tellurium vapor.

The advent of the various analytical techniques for qualitative and quantitative analysis has been reviewed previously [3–12]. The main points are summarized in the following with particular emphasis on progress during recent years.

(i) Homocyclic molecules

It can be seen from Fig. 24 that Raman spectra of sulfur rings are very characteristic, reflecting the ring size, molecular symmetry and bond length pattern [3–6]. Therefore, vibrational spectroscopy is a suitable means for detecting individual molecular species even in mixtures. Qualitative [304] and quantitative [305] Raman spectroscopy have been utilized in solving the long-standing question of the molecular composition of liquid sulfur as a function of temperature (for a historical review of research on liquid sulfur, see [306]). Upon melting, S_8 decomposes and forms homocyclic sulfur molecules of other ring sizes, mainly S_6 and S_7 well in accord with the concentration of hypothetical S_π deduced from Raoult's law [305,306].

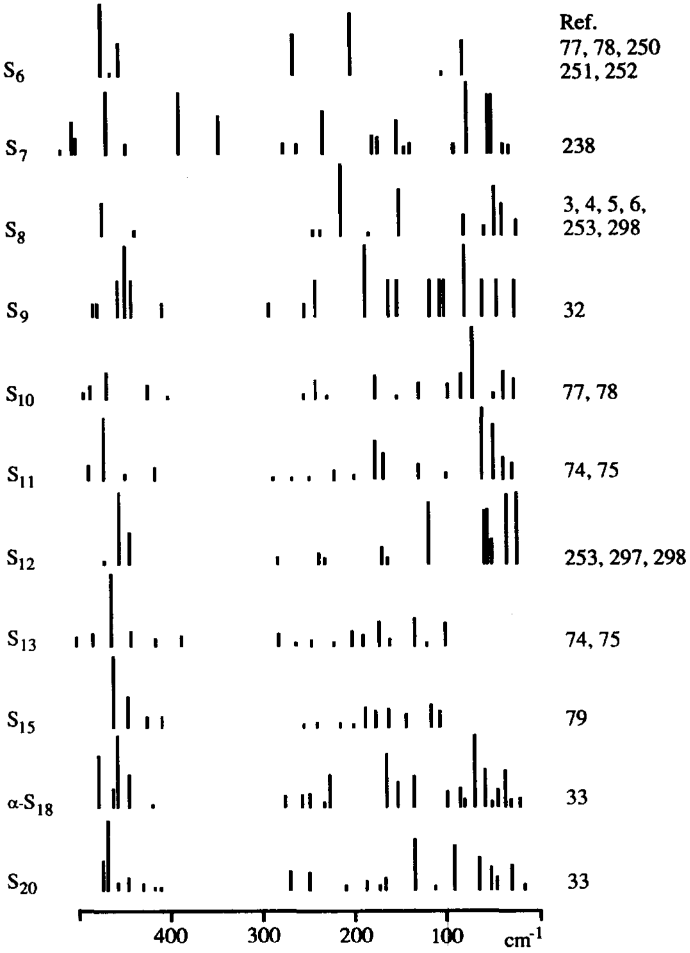

Fig. 24. Raman spectra of homocyclic sulfur species.

Reversed phase HPLC is perhaps the most convenient means to detect homocyclic sulfur and selenium species in molecular mixtures [3–6,307–311] and it has become a routine tool in monitoring chemical reactions involving chalcogen rings. For instance, it was possible with HPLC to verify the Raman spectroscopic conclusions about the composition of sulfur melt [312]. Furthermore, HPLC investigations yielded more accurate quantitative data on the relative concentrations of the various homocyclic sulfur species present in the melt.

Mass spectrometry has yielded information about the composition of sulfur and selenium vapor as a function of temperature (for reviews, see [3–6] and [7–9] for sulfur and selenium, respectively). S_8 is the main component of sulfur vapor up to ca. 800°C with the relative content of smaller molecules increasing with temperature. It seems apparent that molecules larger than S_5 are rings [280]. Recent Raman spectroscopic studies of sulfur vapor [213] over a wide temperature and pressure range have indicated that at least eight different species can be observed through their characteristic Raman lines. These comprise cyclic S_8, S_7 and S_6 and open chain species S_3 and S_2. In addition, there are indications for the presence of two conformational isomers of S_4. Several relationships have been proposed for the correlation of Raman measurements with the thermodynamic properties of sulfur vapor. S_7 is found to be a dominating species in the sulfur vapor at 600–1000 K.

(ii) Heterocyclic molecules

It has been shown above that ^{77}Se NMR is a powerful tool for the identification of discrete molecular species from CS_2 solutions of the quenched sulfur-selenium melts [226] and the melts themselves at 135°C [227]. The peak intensities can conveniently be used in the semiquantitative determination of the relative contents of Se_nS_{8-n} rings. It seems that the compositions are only governed by the total selenium content of the initial sulfur–selenium mixtures. The NMR spectra of the melts also show resonances due to the polymeric material. These resonances can be interpreted in terms of random distribution of various chalcogen fragments governed by the overall elemental composition [227]. The CS_2 solutions do not show resonances due to the polymers, since polymeric material is insoluble in CS_2.

The NMR data of the melts and their CS_2 solutions (see Table 11) indicate that SeS_7 and 1,2-Se_2S_6 are the main components in all samples up to 40 mol% of initial selenium content comprising the range 93–60 mol% [226,227]. It is also seen that the concentration of the species decreases as the selenium content in the ring increases. It is interesting to note that for a given chemical composition the isomer with all selenium atoms adjacent to each other (i.e. $\mathbf{A}_{1-8}$) is the most abundant. This observation is in agreement with the earlier Raman spectroscopic deductions [48,228]. The density functional calculations of Jones and Hohl [242] have shown that for Se_2S_6 and Se_6S_2 rings the isomers with all selenium and all sulfur atoms adjacent to each other indeed are energetically more stable than the isomers with more than two Se–S bonds. Based on the rela-

TABLE 11

The relative distribution of Se_nS_{8-n} species in selective reaction mixtures as a function of initial selenium content[a]

Species		CS$_2$ solution of the quenched melt [226]				Sulfur-selenium melt [227]				Reaction of KI with Se$_2$Cl$_2$/ SCl$_2$ [67]	Reaction of KI with Se$_2$Cl$_2$/S$_2$Cl$_2$								
											[67]						[68]		
		10	30	35	40	5	15	25	35	50	20	25	33	50	67	80	33[b]	33[c]	33[d]
SeS$_7$		70.5	47.0	39.0	40.0	82	61	47	38	–	11	8	5	15	27	24	–	0	4
Se$_2$S$_6$	**A$_2$**	17.0	23.5	20.0	20.0	11	15	20	19	11	51	48	34	33	34	32	25	14	24
	B$_2$	2.5	3.5	3.0	2.5	3	4	5	5	3	14	12	7	6	5	5	15	3	3
	C$_2$	2.0	2.5	3.0	2.0	1	2	3	3	17	9	12	13	6	3	3	18	1	4
	D$_2$	4.0	4.0	3.5	3.5	2	5	5	5	8	5	5	7	8	5	5	–	0	4
Se$_3$S$_5$	**A$_3$**	4.5	8.0	11.5	10.5	1	5	7	9	18	2	5	13	14	10	12	11	14	25
	B$_3$	–	2.0	3.0	4.0	–	3	4	5	4	–	2	4	4	3	3			
	C$_3$	–	2.5	3.5	3.5	–	3	4	5	15	7	6	7	4	3	4	31	62	18
Se$_4$S$_4$	**A$_4$**	–	3.5	6.0	5.5	–	2	2	4	7	–	1	4	4	3	4	–	0	11
	B$_4$	–	1.0	2.0	2.0	–	–	1	3	4									
	D$_4$	–	0.5	1.0	1.0	–	–	–	–	2	–	1	1	–	–	–	–	1	0
	G$_4$	–	<0.5	1.0	0.5	–	–	<0.5	1	–	–	–	–	–	–	–	–	4	2
Se$_5$S$_3$	**A$_5$**	–	1.5	2.5	3.0	–	–	<0.5	2	5	–	–	2	2	2	2	–	0	9
Se$_6$S$_2$	**A$_6$**	–	0.5	1.0	1.5	–	–	<0.5	1	2	–	–	1	1	1	2			
Se$_8$		–	~0.5	<0.5	0.5	–	<0.5	<0.5	<0.5	2	–	–	1	1	2	3			

[a] Initial molar content of selenium in the total amount of the two chalcogen elements.
[b] Freshly prepared reaction mixture after removal of iodine, recording time 5 h.
[c] Freshly prepared solution of orange crystals (obtained upon cooling) in CS$_2$.
[d] The same solution as in c, but after standing at 20°C for 6 months.

tionship between the bond length and bond strength [313], the total binding energy can be expressed in terms of the binding energies of the different types of bonds in the molecule. In 1,2-Se_2S_6 (**A_2**) there are one Se–Se bond, two Se–S bonds and five S–S bonds. Therefore, the total binding energy E_{A_2} depends on the bond contributions as follows:

$$E_{A_2} = E_{SeSe} + 2E_{SeS} + 5E_{SS}$$

In the three remaining isomers (**B_2**, **C_2** and **D_2**), there are four Se–S bonds and four S–S bonds. They are expected to have the same energies:

$$E_{B_2\text{–}D_2} = 4E_{SeS} + 4E_{SS}$$

Therefore the energy difference between **A_2** and **B_2–D_2** can be expressed as follows:

$$\Delta E = E_{A_2} - E_{B_2\text{–}D_2} = E_{SeSe} + E_{SS} - 2E_{SeS}$$

A_2 has been estimated to be 7.4 kJ mol^{-1} lower in energy than **B_2–D_2** [242]. This is consistent with the calculated endothermic transformation of one S–S bond and one Se–Se bond into two Se–S bonds [121,122] and is in agreement with the experimental evidence [124,125]. The same arguments can be applied to the isomers of Se_6S_2 (**A_6–D_6**). These results enable the prediction that, in given chemical composition, the isomer with all sulfur and selenium atoms adjacent to each other is the most stable one [242].

Steudel et al. [314] have made a detailed reversed-phase HPLC study of species extracted from quenched sulfur-selenium melts of two elemental compositions (molar ratio S/Se = 8.7 and 0.33). Linear relationships have been derived for the dependence of retention on the ring size, on the number of selenium atoms, and on the number of heteronuclear bonds in the ring molecule and allow for the prediction of retention times of all selenium sulfide heterocycles of ring sizes 6–12. The two chromatograms and the assignment of the signals are shown in Fig. 25. In general, there seems to be a fair agreement between the HPLC [314] and NMR results [226,227].

It is seen from Fig. 24, however, that the assignment of HPLC peaks is not always unambiguous. The retention indices are often very close together indicating that the signals due to different molecular species may potentially overlap. For instance, peak number 10 of Fig. 25 at the retention time of 9.41 min has been assigned to eight species [314]: S_8 (retention index RS = 793), 1,2-Se_2S_6 (RS = 794), 1,2,4- and 1,2,5-Se_3S_5 (RS = 785) and 1,2,3,5-, 1,2,3,6-, 1,2,4,5-, and 1,2,5,6-Se_4S_4 (RS = 797). The combination of HPLC data with ^{77}Se NMR spectroscopic results helps to remove the ambiguity in most cases. The power of HPLC is its possibility for a quick detection of very small concentrations thus enabling an easier observation of heterocyclic selenium sulfide molecules of ring sizes other than eight that often are short-lived and are thus difficult to detect with the comparatively slower technique of ^{77}Se NMR spectroscopy.

The distribution of Se_nS_{8-n} species produced in the reaction of S_nCl_2/Se_2Cl_2 mixtures of varying composition with KI has been thoroughly investigated both with HPLC

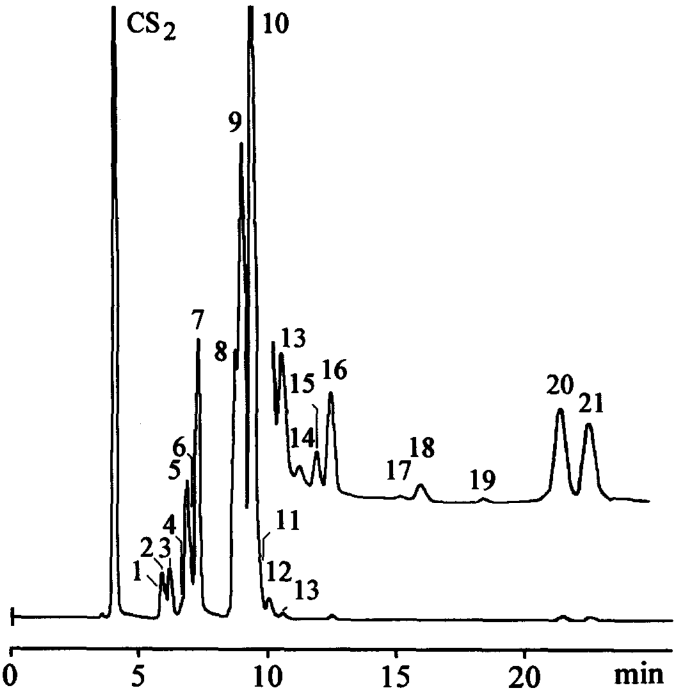

Fig. 25. Chromatogram of the CS_2 extract of the quenched sulfur-selenium melt (initial molar ratio S/Se = 8.7). The upper trace was recorded with twenty-fold increase of sensitivity [314] (© Verlag der Zeitschrift für Naturforschungen).

[66,68] and ^{77}Se NMR [67,68]. On the basis of their pioneering HPLC study, Steudel and Strauss [66] concluded that the reaction of SCl_2 and Se_2Cl_2 (molar ratio 2:1) with KI produced the complete homologous series of eight-membered ring molecules with selenium atoms adjacent to each other (A_1–A_8). The ^{77}Se NMR data [67,68] give a partial verification of these conclusions with two clear differences. There is no evidence in the NMR spectra of the signal due to SeS_7 (A_1) expected at ca. 700 ppm [226].

The reaction mixture also contains significant amounts of species with isolated selenium atoms [67,68] consistent with the existence of $SeSCl_2$ in equilibrium with S_2Cl_2 and Se_2Cl_2 [68,106] as described above.

Steudel et al. [68] have also investigated whether a prolonged standing of the CS_2 solution from the reaction of S_2Cl_2–Se_2Cl_2 (molar ratio 2:1) with KI has an effect on the product distribution (see Table 11). The fresh sample was said to decompose during 6 months at room temperature with formation of new Se_nS_{8-n} species. Even though the authors do not give parameters of their ^{77}Se NMR experiments, it is likely that the accumulation time of 5 h in the freshly prepared solution provides insufficient signal-to-noise for the detection of the minor species. Indeed, the reported chromatogram [68] of the same freshly prepared solution shows the presence of several minor species [for instance

1,2,3,4-Se_4S_4 (A_4), 1,2,3,4,5-Se_5S_3 (A_5)] and is in better agreement with the earlier NMR spectrum [67] recorded for a similar preparation also immediately after the synthesis, but with a long acquisition time. In any case, it has to be remembered that the relative compositions given in Table 11 are only semiquantitative and thus do not allow for detailed conclusions on the small changes in concentrations of the selenium sulfide rings.

(iii) Chalcogen ring interconversion

Compounds containing cumulated S–S bonds undergo facile interconversion reactions in solution and in the molten state. Some examples are the solid state decomposition of unstable homocyclic sulfur molecules with the formation of stable S_8 [315], the decomposition of S_8 in the molten state or in organic solvents [312,316], the polymerization and depolymerization of liquid sulfur [315], the disproportionation of organic polysulfides R_2S_n with the formation of R_2S_{n+1} and R_2S_{n-1} [317,318], and the vulcanization of rubber [319].

Similar interconversion reactions have also been observed for selenium. When Se_8 is dissolved in CS_2, an equilibrium between Se_6, Se_7 and Se_8 is rapidly set up [311]. In the saturated solution (8–10^{-3} mol dm^{-3} Se), there is 7.7 mol% of Se_6, 15.4 mol% of Se_7, and 76.4 mol% of Se_8, while the thousand-fold dilution increases the relative concentration of Se_6 and Se_7 at the expense of Se_8 (34.8 mol% Se_6, 21.7 mol% Se_7 and 43.5 mol% Se_8) [311]. The corresponding decomposition of S_8 to S_6 and S_7 is much slower in CS_2 and

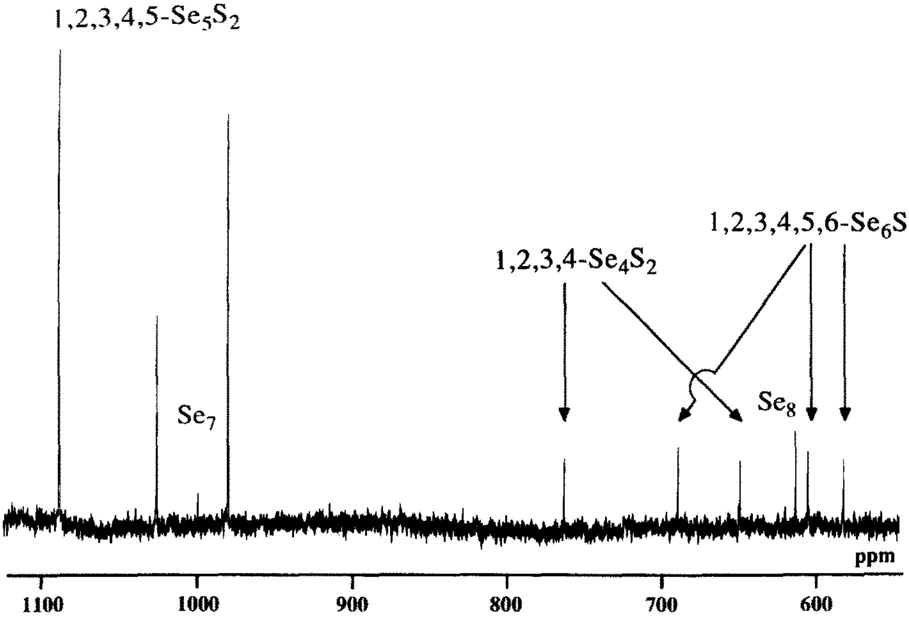

Fig. 26. Natural-abundance ^{77}Se NMR spectrum of the CS_2 solution of 1,2,3,4,5-Se_5S_2 after 1 day of decomposition [233] (© American Chemical Society).

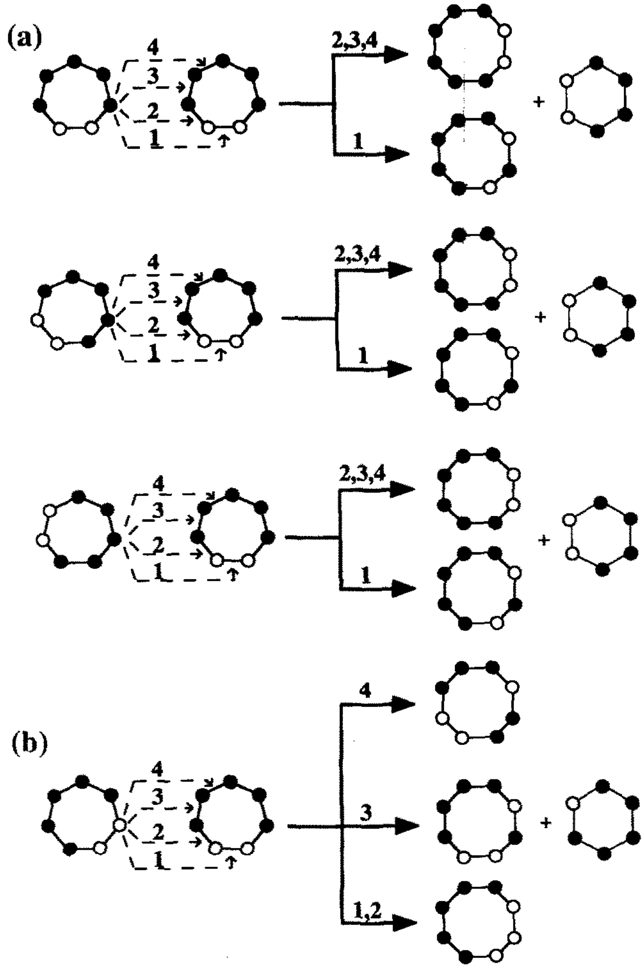

Fig. 27. Possible pathways for chalcogen atom transfer in the interconversion of 1,2,3,4,5-Se_5S_2. (a) Selenium atom transfer, (b) sulfur atom transfer [233] (© American Chemical Society).

requires heating in sealed ampoules to 130–150°C [316]. The equilibrium mixtures were reported to contain 1–2 mol% of S_6, 5–7 mol% S_7 and 91–94 mol% S_8. Tebbe et al. [320] have reported that the equilibrium is instantaneously established in acetonitrile. The contents of S_6 and S_7, however, were much smaller (0.4 and 0.8 mol%, respectively).

The complicated mixtures of selenium sulfides formed with most preparative routes (see Table 2) most likely result from interconversion reactions of the type described above. For instance, upon reaction of $[Ti(C_5H_5)_2S_5]$ with Se_2Cl_2 a seven-membered 1,2-Se_2S_5 is formed, but in CS_2 it decomposes with the formation of SeS_5 and 1,2,3-Se_3S_5 [81,82]. All reaction products could be identified by vibrational [81,82,243] and by ^{77}Se NMR [244] spectroscopy. An analogous reaction takes place when $[Ti(C_5H_5)_2S_5]$ is treated with $SeBr_2$ (a mixture of $SeBr_4$ and Se) [83]. In addition to the three products mentioned above, the formation of 1,2- and 1,7-isomers of Se_2S_{10}, 1,2- and 1,5-isomers of Se_2S_6, 1,2,5,6-Se_4S_4, and S_{10} were reported.

Because the decomposition of 1,2,3,4,5-Se_5S_2 is slower than that of 1,2-Se_2S_5, it can be followed in more detail [85,233]. The freshly prepared samples showed only resonances due to 1,2,3,4,5-Se_5S_2, but when the samples were allowed to stand in the CS_2 solution, resonances due to 1,2,3,4-Se_4S_2 and 1,2,3,4,5,6-Se_6S_2 appeared [233] (see Fig. 26). When preparing the sample using ^{77}Se-enriched selenium, the decomposition products could be identified on the basis of their coupling patterns (see Table 7).

All of the examples listed above involve a chalcogen atom transfer. This can be shown schematically for 1,2,3,4,5-Se_5S_2 [233] (see Fig. 27). The possibilities comprise a sulfur or a selenium atom transfer from one seven-membered ring molecule to the other. As seen from Fig. 27, all possible selenium atom transfer reactions produce two different sets of compounds. The six-membered ring 1,2,3,4-Se_4S_2 is formed in every case, but the eight-membered product is either 1,2,3,4,5,6-Se_6S_2 or 1,2,3,4,5,7-Se_6S_2 depending on where in the molecule the selenium atom is inserted. In the case of sulfur atom transfer, Se_5S and 1,2,3,4,5-, 1,2,3,4,6-, or 1,2,3,5,6-isomers of Se_5S_3 are formed depending on the point of insertion [233]. Since the ^{77}Se NMR spectroscopic evidence only indicates the

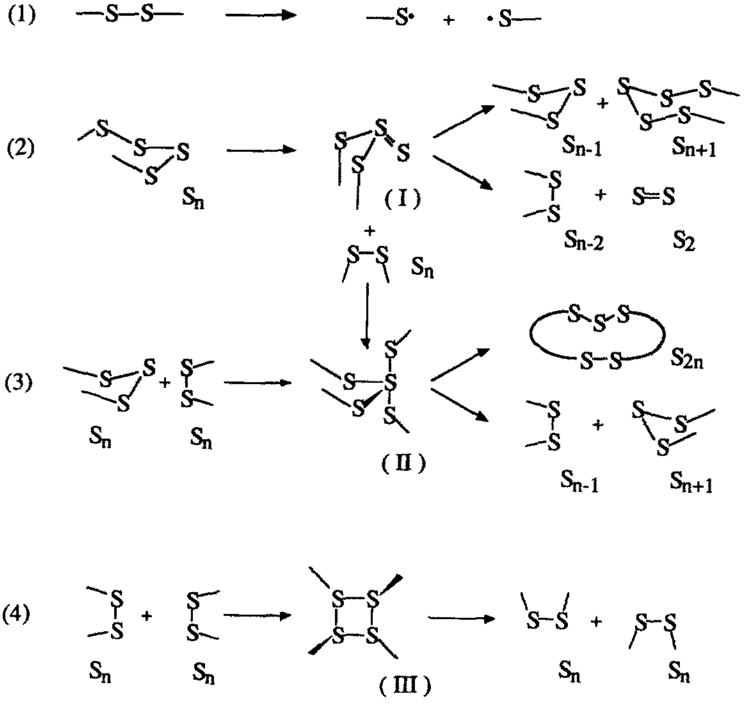

Fig. 28. Suggested intermediates in the interconversion reactions of molecules containing cumulated sulfur–sulfur bonds [333].

formation of 1,2,3,4-Se_4S_2 and 1,2,3,4,5,6-Se_6S_2, a selenium atom transfer reaction is inferred with the points of insertion not in the S–S bond of 1,2,3,4,5-Se_5S_2.

Similar alternatives in the decomposition of 1,2-Se_2S_5 result in the formation of SeS_5 and 1,2,3-, 1,2,4- or 1,2,5-isomers of Se_3S_5 in the case of selenium atom transfer, and 1,2-Se_2S_4 and 1,2- or 1,3-isomers of Se_2S_6 in the case of sulfur atom transfer. The spectroscopic evidence [81,82] again point towards the selenium atom transfer with the insertion not in any of the S–S bonds in the molecule.

The mechanism of chalcogen ring interconversion reactions is not known. Several pathways that have been suggested are summarized in Fig. 28 (for a review, see [3]). It is also possible that there are several competing mechanisms depending on the reaction conditions. In view of the similarity of the electronic structures of the S–S, Se–S and Se–Se bonds [121,122] (see also Fig. 1), it is possible that the interconversion reactions involving sulfur and selenium rings proceed in a similar manner. The pathways are speculative due to the lack of rigorous experimental evidence.

Radicals have not been detected for sulfur in organic solvents or in the molten state below the polymerization threshold at ca. 160°C [321–323], rendering the homolytic cleavage rather unlikely in these conditions. Steudel [3] has therefore suggested that hypervalent intermediates of the types

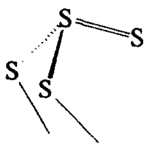

and

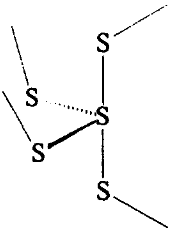

(I) (II)

could be involved in the interconversion. He has also discussed the structure and properties of amorphous selenium in terms of such intermediates [324]. Many species related structurally to both types of intermediates have been prepared or identified spectroscopically. For instance, F_2SS [325], Cl_2SS [326,327], Br_2SS [326] and $(RO)_2SS$ [328] are related to structure **I**. In fact, F_2SS is more stable than the FSSF isomer [325], but Cl_2SS and Br_2SS have only been detected in argon matrices at 9 K after the photochemical isomerization of unbranched disulfur dihalides [326].

Structure **II** can be exemplified by R_2SCl_2 [329,330], $FSSF_3$ and $FSSSF_3$ [331] as well as several other organic sulfuranes [332]. The insertion of R_2S into covalent single bonds proceeds smoothly even at low temperatures [329,332]:

$$R_2S + Cl_2 \rightarrow R_2SCl_2$$

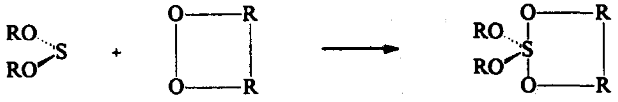

Recently, the geometries and energetics of formation of different suggested interconversion intermediates shown in Fig. 28 have been studied with ab initio MO techniques using the reactions of the first four members of the sulfane series H_2S_n (n = 1–4) as models [333]. The geometry optimization involved 4-31G* basis sets and yielded good agreement with experimental geometries where available. The energetics of formation of the hypervalent intermediates of Fig. 28 are exemplified by $(HS)_2SS$ (type I) and $H_2S(SSH)_2$ (type II). Their energy of formation from the starting sulfanes was calculated using the MP2/6-31G//4-31G and MP3/6-31G//4-31G levels of theory and compared to the homolytic cleavage of the S–S bond. The results are summarized in Table 12. The hypervalent intermediates have also been studied with SINDO1 [239].

The thiosulfoxide type intermediate (structure I) seems to be energetically competitive for the homolytic cleavage of cumulated S–S bonds. Such species have often been suggested as intermediates for reactions of compounds containing S–S bonds [335,336]. Mulliken population analysis [333] indicates that there is a considerable negative charge (–0.4 e) on the terminal sulfur atom. Therefore, the intermediate of the type I is expected to be a strong nucleophile. The bond scission of the attacked molecule results in the net sulfur atom transfer [333].

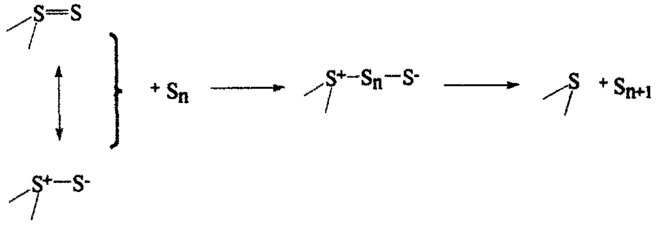

Steudel et al. [83] have discussed the pathway for dimerization of SeS_5 in similar terms:

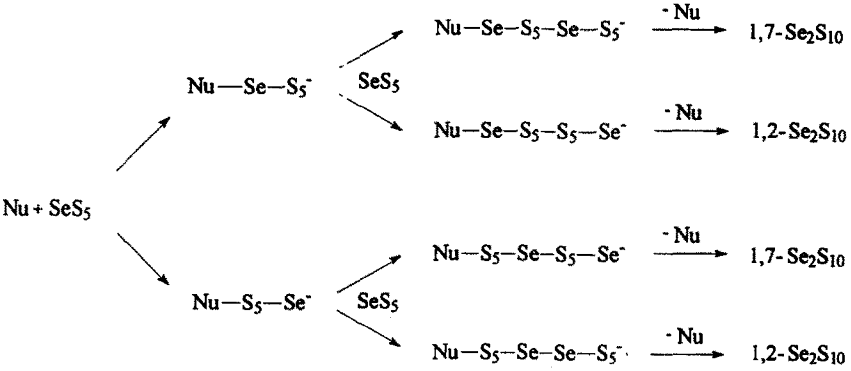

The nucleophile can be thought to be either a contracted chalcogen ring with an exocyclic thiosulfoxide type structure, or an impurity. The HPLC and Raman observation that both twelve-membered Se_2S_{10} isomers are formed in the reaction excludes the

TABLE 12

Energies of formation of the selected interconversion intermediates (in kJ mol^{-1}) [333]

Reaction	MP2	MP3	Exptl.
$HSSH \rightarrow 2HS^{\cdot}$	229.3	221.3	276.1[a]
$HSSSSH \rightarrow 2HSS^{\cdot}$	153.1	138.9	148.1[b]
$HSSSSH \rightarrow (HS)_2SS$	123.4	132.2	
$HSH + HSSSSH \rightarrow H_2S(SSH)_2$	189.5	205.4	

[a] Ref. 194.
[b] Ref. 334.

alternative conceivable pathway that Se_2S_{10} is produced directly from the starting $[Ti(C_5H_5)_2S_5]$ and SeS_5 [83]. This latter route should produce only 1,7-Se_2S_{10}.

The formation of the sulfurane type intermediate **II** is energetically comparable to the dissociation energy of an isolated S–S bond and therefore not quite an attractive alternative for homolytic cleavage of the cumulated S–S bond [333]. Electronegative substituents, however, are known to stabilize the four-coordinated sulfur species (cf. SF_4 [337,338], R_2SCl_2 [329] and $(RO)_2S(OR)_2$ [332]). It is therefore conceivable that with longer sulfur chains, this type of intermediate will also play a role in the interconversion. It is certainly easy to explain a chalcogen atom transfer with this scheme [82]:

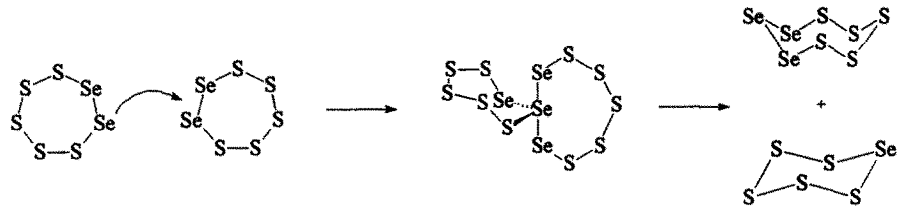

Neither scheme explains the pathway of interconversion when the ring size does not change. This kind of interconversion, however, is observed in the CS_2 solutions of selenium sulfide rings. For instance, when the solution containing the decomposition products of 1,2,3,4,5-Se_5S_2 is allowed to stand, a rich mixture of different Se_nS_{7-n}, Se_nS_{8-n} and possibly Se_nS_{6-n} species is formed in addition to the initial 1,2,3,4-Se_4S_2 and 1,2,3,4,5,6-Se_6S_2 [86].

The polymerization of sulfur rings in the melts has been extensively studied (for a review see [306]). More recently, Steudel et al. [315] have studied the polymerization and depolymerization of various homocyclic sulfur molecules with HPLC, DSC and Raman spectroscopy. The results were discussed in terms of the radical chains. The homolytic cleavage of the S_6 and S_7 ring molecules was concluded to play an important role in the polymerization [315,334]. Geyer et al. [339] report a photolysis study of supercooled cyclooctasulfur droplets. The polymerization was found to be dependent on the wavelength of radiation. They also observed photoinduced desorption of cyclooctasulfur thin films with the rate of desorption dependent on the light intensity and concluded that the desorption process was not purely thermal.

The polymerization of sulfur-selenium phases has been investigated by the appearance of phase method, DTA and DSC [340]. The complete liquid miscibility of sulfur and selenium was verified and it was explained in terms of the equilibrium copolymerization theory. The addition of selenium into sulfur was found to lower the polymerization threshold. The eutectoid proposed by Ringer [341] in the sulfur-rich part of the system was not detected [340].

Steudel et al. [294] have studied the photochemical decomposition of CS_2 solutions of pure S_6, S_7, S_8, S_{10} and S_{12} at 15°C on irradiation and determined the soluble products by reversed phase HPLC. A mixture of sulfur homocycles S_n with S_6, S_7 and S_8 as the main species was formed in each case. The existence of radical chains is also quite possible in these reactions. The low-temperature irradiation of orthorhombic S_8 was also studied with ESR and the nature of radicals formed was discussed [293]. The impetus for the work comes from the hypothesis that the color of one of the Jovian moons, Io, is a consequence of elemental sulfur on the surface [342]. It was observed that while S_8 is white at 77 K, it turns intensely yellow upon irradiation with UV radiation. The color was explained in terms of an absorption at 430 nm possibly caused by a chain-like sulfur diradical. It was found to decompose at 260 K with the formation of polymeric sulfur. Other sulfur homocycles also showed analogous behavior. It was suggested that the yellowish color of Io is caused by the effects of solar radiation on elemental sulfur. The color is possibly modified by deposits of SO_2 frosts and volcanic ash [342].

J. CONCLUSIONS

The chemistry of chalcogen elements has long been known to be extensive. During the last 20 years the development of modern analytical techniques has shown that the elemental system of sulfur consists of a large number of homocyclic as well as open chain molecules. The molecular variety for selenium and tellurium is narrower. The existence of Se_6, Se_7 and Se_8, with the molecular structures similar to the analogous sulfur species, is well established. For tellurium, the existence of cyclic Te_8 has been suggested, but awaits unambiguous confirmation.

The binary system of sulfur and selenium is very complex and is composed of numerous heterocyclic and polymeric species. The joint application of vibrational spectroscopy, HPLC and ^{77}Se NMR spectroscopy seems to be the key to the identification of discrete molecular species in the mixtures formed by different routes. ^{125}Te NMR has provided evidence for the existence of heterocyclic tellurium sulfides and tellurium selenium sulfides.

In recent years, the research emphasis has shifted from purely structural studies towards understanding the interconversion reactions between the different molecular species. The rapid development of computational techniques has enabled accurate theoretical studies to be performed even on large molecules. The comparison of geometries and electronic structures of the chalcogen–chalcogen bonds has shown that S–S, Se–S and Se–Se bonds are rather similar. Tellurium-containing bonds are more at variance. It is therefore possible to study the interconversion of sulfur rings by inserting selenium atoms in the homocyclic molecule as chemical labels. The interconversion reactions can be monitored with NMR, the products identified and new insights into the decomposition pathways gained.

It is interesting to note that despite the structural similarities between the three elements, there are also differences. Cyclooctasulfur is the thermodynamically stable molecular form and polymeric sulfur is unstable at NTP, but the converse is true for selenium and tellurium. Even though the molecular structures of analogous sulfur and selenium rings are similar, the packing of the molecules does not result in different crystal structures. Generally, the intermolecular distances in selenium allotropes are shorter than in sulfur allotropes. This has been explained by the greater polarizability of selenium compared to sulfur.

The structural differences are of course reflected in the properties. Sulfur, for instance, is an insulator, while selenium and tellurium are semiconductors. Studies of heterocyclic selenium sulfides and tellurium sulfides are therefore important not only because of the structural similarities. They also provide a bridge between the properties of insulating materials and semiconductors. The question to motivate sulfur and selenium research could well be: if sulfur and selenium are so similar, why are they so different?

ACKNOWLEDGMENTS

We are indebted to Professor T. Chivers for his helpful comments in the preparation of the manuscript. Financial support from the Academy of Finland is gratefully acknowledged.

REFERENCES

1 M.G. Barker, Coord. Chem. Rev., 49 (1983) 383.
2 M.G. Barker, Coord. Chem. Rev., 103 (1990)162.
3 R. Steudel, Top. Curr. Chem., 102 (1982) 149.
4 R. Steudel, in A. Müller and B. Krebs, Eds., Sulfur, its Significance for Chemistry, for the Geo-, Bio-, and Cosmosphere and Technology, Elsevier, Amsterdam, 1984, p. 3.
5 R. Steudel, Nova Acta Leopoldina, 59 (1985) 231.
6 R. Steudel, in I. Haiduc and D.B. Sowerby, Eds., The Chemistry of Inorganic Homo- and Heterocycles, Vol. 2, Academic Press, London, 1987, p. 737.
7 Gmelin Handbuch der anorganischen Chemie, Selen Erg. Band A2, 8th edition, Springer-Verlag, Berlin,1980, p. 179.
8 R. Steudel and E.-M. Strauss, Adv. Inorg. Chem. Radiochem., 28 (1984) 135.
9 R. Steudel and E.-M. Strauss, in I. Haiduc and D.B. Sowerby, Eds., The Chemistry of Inorganic Homo- and Heterocycles, Vol. 2., Academic Press, London, 1987, p. 769.
10 R. Steudel and R. Laitinen, Top. Curr. Chem., 102 (1982) 177.
11 Gmelin Handbuch der anorganischen Chemie, Selenium, Suppl. B2, 8th edition, Springer-Verlag, Berlin, 1984, p. 280.

12 R. Laitinen, Acta Chem. Scand., 41A (1987) 361.
13 R.J. Gillespie, Chem. Soc. Rev., 8 (1979) 315.
14 T. Klapötke and J. Passmore, Acc. Chem. Res., 22 (1989) 234.
15 J. Passmore, Stud. Inorg. Chem., 14 (1992) 373.
16 P. Böttcher, Angew. Chem., 100 (1988) 781; Angew. Chem. Int. Ed. Engl., 27 (1988) 759.
17 M.G. Kanatzidis and S.-P. Huang, Inorg. Chem., 28 (1989) 4667.
18 D. Fenske, G. Kräuter and K. Dehnicke, Angew. Chem., 102 (1990) 420; Angew. Chem., Int. Ed. Engl., 29 (1990) 390.
19 R. Zagler and B. Eisenmann, Z. Naturforsch., 46b (1991) 593.
20 Gmelin Handbuch der anorganischen Chemie, Schwefel Erg. Band 3, 8th edition, Springer-Verlag, Berlin,1980, p. 3.
21 R. Steudel, Comments Inorg. Chem., 1 (1982) 313.
22 R. Steudel, Phosphorus Sulphur, 23 (1985) 33.
23 M. Draganjac and T.B. Rauchfuss, Angew. Chem., 97 (1985) 745; Angew. Chem., Int. Ed. Engl., 24 (1985) 742.
24 A. Müller and E. Diemann, Adv. Inorg. Chem., 31 (1987) 89.
25 M.G. Kanatzidis, Comments Inorg. Chem., 10 (1990)161.
26 J.W. Kolis, Coord. Chem. Rev., 105 (1990)195.
27 M.A. Ansari and J.A. Ibers, Coord. Chem. Rev., 100 (1990) 223.
28 B. Meyer, Sulfur, Energy, and Environment, Elsevier, Amsterdam, 1977, 448 p.
29 E.M. Elkin, in M. Grayson and D. Eckroth, Eds., Kirk-Othmer Encyclopedia of Chemical Technology, Vol. 20, Wiley, New York, 1982, p. 575.
30 M. Schmidt and H.-D. Block, Angew. Chem., 79 (1967) 944; Angew. Chem., Int. Ed. Engl., 6 (1967) 955.
31 R. Steudel and H.-J. Mäusle, Angew. Chem., 90 (1978) 54; Angew. Chem., Int. Ed. Engl., 17 (1978) 56.
32 R. Steudel and H.-J. Mäusle, Z. Anorg. Allg. Chem., 478 (1981) 156.
33 R. Steudel and H.-J. Mäusle, Angew. Chem., 91 (1979) 165; Angew. Chem., Int. Ed. Engl., 18 (1979) 152.
34 R. Steudel and B. Holz, Z. Naturforsch., 43b (1988) 581.
35 R.D. Burbank, Acta Crystallogr., 4 (1951) 140.
36 R.D. Burbank, Acta Crystallogr., 5 (1952) 236.
37 G.B. Abdullayev, Y.G. Asadov and K.P. Mamedov, in W.C. Cooper, The Physics of Selenium and Tellurium, Pergamon Press, Oxford, 1969, p. 179.
38 S. Izima, J. Taynai and M.-A. Nicolet, in W.C. Cooper, ed., The Physics of Selenium and Tellurium, Pergamon Press, Oxford, 1969, p. 199.
39 Y. Miyamoto, Jpn. J. Appl. Phys., 16 (1977) 2257.
40 K. Nagata, H. Tashiro and Y. Miyamoto, Jpn. J. Appl. Phys., 20 (1981) 2265.
41 K. Nagata and Y. Miyamoto, Jpn. J. Appl. Phys., 23 (1984) 704.
42 J.E. Fergusson, G.M. Pratt, G.A. Rodley and C.J. Wilkins, J. Inorg. Nucl. Chem., 24 (1962) 157.
43 L.L. Hawes, Nature, 198 (1963)1267.
44 R. Cooper and J.V. Culka, J. Inorg. Nucl. Chem., 27 (1965) 755.
45 R. Cooper and J.V. Culka, J. Inorg. Nucl. Chem., 29 (1967) 1217.
46 C.R. Ailwood and P.E. Fielding, Aust. J. Chem., 22 (1969) 2301.
47 R. Laitinen, L. Niinistö and R. Steudel, Acta Chem. Scand., A33 (1979) 737.
48 H.H. Eysel and S. Sunder, Inorg. Chem., 18 (1979) 2626.
49 R. Cooper and J.V. Culka, J. Inorg. Nucl. Chem., 29 (1967)1877.
50 T. Chivers, R.S. Laitinen, K.J. Schmidt and J. Taavitsainen, Inorg. Chem., 32 (1993) 337.

51 K. Nagata, H. Hayashi and M. Miyamoto, Fukuoka Univ. Sci. Rep., 18 (1988) 23.

52 K. Nagara, H. Hayashi and Y. Miyamoto, Fukuoka Univ. Sci. Rep.,18 (1988) 35.

53 T. Nakagawa, Bull. Chem. Soc. Jpn., 48 (1975) 641.

54 F. Fehér, in G. Brauer, Ed., Handbuch der Präparativen Anorganischen Chemie, Erster Band, 3rd edition, Ferdinand Enke Verlag, Stuttgart,1975, p. 410.

55 J. Weiss, Z. Anorg. Allg. Chem., 435 (1977)113.

56 R. Boudet, Ann. Chim. (Paris), 10 (1955)178.

57 M. Schmidt and E. Wilhelm, Inorg. Nucl. Chem. Lett., 1 (1965) 39.

58 M. Schmidt and E. Wilhelm, Angew. Chem., 78 (1966) 1020; Angew. Chem., Int. Ed. Engl., 5 (1966) 964.

59 M. Schmidt, G. Knippschild and E. Wilhelm, Chem. Ber., 101 (1968) 381.

60 M. Schmidt, E. Wilhelm, T. Debaerdemaeker, E. Hellner and A. Kutoglu, Z. Anorg. Allg. Chem., 405 (1974) 153.

61 T. Debaerdemaeker, E. Hellner, A. Kutoglu, M. Schmidt and E. Wilhelm, Naturwissenschaften, 60 (1973) 300.

62 R. Cooper and J.V. Culka, J. Inorg. Nucl. Chem., 32 (1970)1857.

63 M. Schmidt and E. Wilhelm, Z. Naturforsch., 25b (1970) 272.

64 H.-J. Mäusle and R. Steudel, Z. Anorg. Allg. Chem., 463 (1980) 27.

65 J. Weiss and W. Bachtler, Z. Naturforsch., 28b (1973) 523.

66 R. Steudel and E.-M. Strauss, Z. Naturforsch., 38b (1983) 719.

67 R.S. Laitinen, P. Pekonen, Y. Hiltunen and T.A. Pakkanen, Acta Chem. Scand. 43 (1989) 436.

68 R. Steudel, B. Plinke, D. Jensen and F. Baumgart, Polyhedron, 10 (1991) 1037.

69 M. Pupp and J. Weiss, Z. Anorg. Allg. Chem., 440 (1978) 31.

70 J. Weiss and M. Pupp, Angew. Chem., 82 (1970) 447; Angew. Chem., Int. Ed. Engl., 9 (1970) 463.

71 J. Weiss and M. Pupp, Acta Crystallogr., Sect. B, 28 (1972) 3653.

72 M. Schmidt, B. Block, H.D. Block, H. Köpf and E. Wilhelm, Angew. Chem., 80 (1968) 660; Angew. Chem., Int. Ed. Engl., 7 (1968) 632.

73 M. Schmidt and E. Wilhelm, J. Chem. Soc., Chem. Commun., (1970) 1111.

74 T. Sandow, J. Steidel and R. Steudel, Angew. Chem., 94 (1982) 782; Angew. Chem., Int. Ed. Engl., 21 (1982) 794.

75 R. Steudel, J. Steidel and T. Sandow, Z. Naturforsch., 41b (1986) 958.

76 J. Steidel, R. Steudel and A. Kutoglu, Z. Anorg. Allg. Chem., 476 (1981) 171.

77 R. Steudel, J. Steidel, T. Sandow and F. Schuster, Z. Naturforsch., 33b (1978) 1198.

78 R. Steudel, J. Steidel and R. Reinhardt, Z. Naturforsch., 38b (1983) 1548.

79 R. Strauss and R. Steudel, Z. Naturforsch., 43b (1988) 1151.

80 R. Steudel and R. Strauss, J. Chem. Soc., Dalton Trans., (1984) 1775.

81 R. Laitinen, N. Rautenberg, J. Steidel and R. Steudel, Z. Anorg. Allg. Chem., 486 (1982) 116.

82 R. Steudel and E.-M. Strauss, Angew. Chem., 96 (1984) 356; Angew. Chem., Int. Ed. Engl., 23 (1984) 362.

83 R. Steudel, D. Jensen and F. Baumgart, Polyhedron, 9 (1990) 1199.

84 M. Pridöhl, R. Steudel and F. Baumgart, Phosphorus, Sulfur, Silicon Relat. Elem., 65 (1992) 169.

85 R. Steudel, M. Papavassiliou, E.-M. Strauss and R. Laitinen, Angew. Chem., 98 (1986) 81; Angew. Chem., Int. Ed. Engl., 25 (1986) 99.

86 P. Pekonen, Y. Hiltunen, R.S. Laitinen and T.A. Pakkanen, Inorg. Chem., 29 (1990) 2770.

87 P. Pekonen, R.S. Laitinen and Y. Hiltunen, J. Chem. Soc., Dalton Trans., (1992) 2885.

88 R. Steudel, D. Jensen and M. Papavassiliou, Phosphorus, Sulfur, Silicon Relat. Elem., 41 (1989) 349.
89 D.M. Giolando, M. Papavassiliou, J. Pickardt, T.B. Rauchfuss and R. Steudel, Inorg. Chem., 27 (1988) 2596.
90 M. Papavassiliou, J. Pickardt and R. Steudel, Phosphorus, Sulfur, Silicon Relat. Elem., 65 (1992) 161.
91 P. Pekonen, E: Haapaniemi and R.S. Laitinen, The 7th National Symposium on Inorganic and Analytical Chemistry, 1992, Program and Abstracts, Department of Chemistry, University of Jyväskylä Research Report No. 40, Jyväskylä, 1992, p. 102.
92 R.S. Laitinen and J. Taavitsainen, University of Oulu, Report Series in Chemistry, 42 (1993) L9.
93 U. Westphal and R. Steudel, Phosphorus Sulfur Silicon Relat. Elem., 65 (1992) 151.
94 Y. Watanabe, Acta Crystallogr., Sect. B, 30 (1974) 1396.
95 A.H.W. Aten, Z. Phys. Chem., 88 (1914) 321.
96 R. Steudel and H.-J. Mäusle, Z. Anorg. Allg. Chem., 457 (1979) 165.
97 O. Foss and J.V. Janickis, J. Chem. Soc., Chem. Commun., (1977) 834.
98 O. Foss and J.V. Janickis, J. Chem. Soc., Dalton Trans., (1980) 624.
99 P. Coppens, Y.W. Yang, R.H. Blessing, W.F. Cooper and F.K. Larsen, J. Am. Chem. Soc., 99 (1977) 760.
100 S.J. Rettig and J. Trotter, Acta Crystallogr., Sect. C, 43 (1987) 2260.
101 L.K. Templeton, D.H. Templeton and A. Zalkin, Inorg. Chem., 15 (1976) 1999.
102 L.M. Goldsmith and C.E. Strouse, J. Am. Chem. Soc., 99 (1977) 7580.
103 P. Cherin and P. Unger, Acta Crystallogr., Sect. B, 25 (1972) 313.
104 R.E. Marsh, L. Pauling and J.D. McCullough, Acta Crystallogr., 16 (1953) 71.
105 R. Steudel, T. Sandow and J. Steidel, Z. Naturforsch., 40b (1985) 594.
106 J.B. Milne, Can. J. Chem., 70 (1992) 693.
107 D.M. Giolando, T.B. Rauchfuss, A.L. Rheingold and S.R. Wilson, Organometallics, 6 (1987) 667 and refs. therein.
108 J.A. Gladysz, J.L. Hornby and J.E. Garbe, J. Org. Chem., 43 (1978) 1204.
109 A. Shaver and J.M. McCall, Organometallics, 3 (1984)1823.
110 V.N. Bogomolov, A.I. Zadorozhnii, V.P. Petranovskii, A.V. Fokin and S.V. Kholodkevich, JETP Lett., 29 (1979) 373.
111 V.N. Bogomolov, A.I. Zadorozhnii, T.M. Pavlova, V.P. Petranovskii, V.P. Podkhalyuzin and A.L. Kholkin, JETP Lett., 31 (1980) 378.
112 B. Meyer, Chem. Rev., 76 (1976) 367.
113 R. Steudel, Angew. Chem., 87 (1975) 683; Angew. Chem., Int. Ed. Engl., 14 (1975) 655.
114 S. Geller and M.D. Lind, Acta Crystallogr., Sect. B, 25 (1969) 2166.
115 M.D. Lind and S. Geller, J. Chem. Phys., 51 (1969) 348.
116 P. Cherin and P. Unger, Inorg. Chem., 6 (1967) 1589.
117 C. Adenis, V. Langer and O. Lindqvist, Acta Crystallogr., Sect. C, 45 (1989) 941.
118 A. Karpfen, Chem. Phys. Lett., 136 (1987) 571.
119 M. Springborg and R.O Jones, J. Chem. Phys., 88 (1988) 2652.
120 P. Birner, H.-J. Köhler, A. Karpfen and H. Lischka, J. Mol. Struct. (Theochem), 226 (1991) 223.
121 R. Laitinen and T. Pakkanen, J. Mol. Struct. (Theochem), 91(1983) 337.
122 R. Laitinen and T. Pakkanen, J. Mol. Struct. (Theochem), 124 (1985) 293.
123 E. Herbst and G. Winnewisser, Chem. Phys. Lett., 155 (1989) 572.
124 T. Maekawa, T. Yokokawa and K. Niwa, Bull. Chem. Soc. Jpn., 46 (1973) 761.

125 J. Drowart and S. Smoes, J. Chem. Soc., Faraday Trans. 2, 73 (1977) 1755.

126 J. Donohue, A. Caron and E. Goldish, J. Am. Chem. Soc., 83 (1961) 3748.

127 J. Steidel, J. Pickardt and R. Steudel, Z. Naturforsch., 33b (1978) 1554.

128 Y. Miyamoto, Jpn. J. Appl. Phys., 19 (1980) 1813.

129 R. Steudel, R. Reinhardt and F. Schuster, Angew. Chem., 89 (1977) 756; Angew. Chem., Int. Ed. Engl., 16 (1977) 715.

130 R. Steudel, J. Steidel, J. Pickardt, F. Schuster and R. Reinhardt, Z. Naturforsch., 35b (1980) 1378.

131 R. Staffel, U. Müller, A. Ahle and K. Dehnicke, Z. Naturforsch., 46b (1991) 1287.

132 J. Dietz, U. Müller, V. Müller and K. Dehnicke, Z. Naturforsch., 46b (1991) 1293.

133 T. Kawada, T. Matsumoto, H. Burzlaff and E. Hellner, Acta Crystallogr., Sect. A, 28 (1972) S61.

134 C. Calvo, R.J. Gillespie, J.E. Vekris and H.N. Ng, Acta Crystallogr., Sect. B, 34 (1978) 911.

135 R.A. Boudreau and H.M. Haendler, J. Solid. State Chem., 36 (1981) 289.

136 R. Steudel, M. Papavassiliou and F. Baumgart, Z. Naturforsch., 46b (1991) 1674.

137 R. Reinhardt, R. Steudel and F. Schuster, Angew. Chem., 90 (1978) 55; Angew. Chem., Int. Ed. Engl., 17 (1978) 57.

138 J. Steidel and R. Steudel, J. Chem. Soc., Chem. Commun., (1982) 1312.

139 A. Kutoglu and E. Hellner, Angew. Chem., 78 (1966) 1021; Angew. Chem. Int. Ed. Engl., 5 (1966) 965.

140 T. Debaerdemaeker and A. Kutoglu, Naturwissenschaften, 60 (1973) 49.

141 T. Debaerdemaeker and A. Kutoglu, Cryst. Struct. Commun., 3 (1974) 611.

142 T. Bjorvatten, Acta Chem. Scand.,16 (1962) 749.

143 T. Bjorvatten, O. Hassel and A. Lindheim, Acta Chem. Scand., 17 (1963) 689.

144 T.W. Hambley, C.L. Raston and A.H. White, Aust. J. Chem., 30 (1977) 1965.

145 R. Laitinen, J. Steidel and R. Steudel, Acta Chem. Scand., A34 (1980) 687.

146 A. Müller, R. Römer, H. Bögge, E. Kricklmeyer, F.W. Baumann and E. Schmitz, Inorg. Chim. Acta, 89 (1984) L7.

147 A. Müller, R. Römer, H. Bögge, E. Kricklmeyer and M. Zimmerman, Z. Anorg. Allg. Chem., 534 (1986) 69.

148 H.W. Roesky, M. Thomas, J. Schrimkowiak, P.G. Jones, W. Pinkert and G.M. Sheldrick, J. Chem. Soc., Chem. Commun., (1982) 895.

149 F.A. Cotton, P.A. Kibala and R.B.W. Sandor, Acta Crystallogr., Sect. C, 45 (1989) 1287.

150 D.L. Hughes, J.D. Lane and R.L. Richards, J. Chem. Soc., Dalton Trans., (1991) 1627.

151 D.R. Salahub, A.E. Foti and V.H. Smith Jr., J. Am. Chem. Soc., 99 (1977) 8067.

152 D. Hohl, R.O. Jones, R. Car and M. Parrinello, J. Chem. Phys., 89 (1988) 6823.

153 J. Kao and N.L. Allinger, Inorg. Chem., 16 (1977) 35.

154 A.A. Palma and N.V. Cohan, Rev. Mex. Fis., 19 (1970) 15.

155 B. Meyer and K. Spitzer, J. Phys. Chem., 76 (1972) 2274.

156 B. Meyer, M. Gouterman, D. Jensen, T.V. Oommen, K. Spitzer and T. Strover-Hansen, Adv. Chem. Ser., 110 (1972) 53.

157 E.-K. Kortela, E. Suoninen, M. Karras and R. Manne, J. Phys. B, Atom. Mol. Phys., 5 (1972) 2032.

158 Z. Slanina, P. Kopacek and S. Beran, Z. Phys. Chem., 267 (1986) 1159.

159 D.J. Miller and L.C. Cusachs, Chem. Phys. Lett., 3 (1969) 501.

160 D.J. Gibbons, Mol. Cryst. Liquid Cryst., 10 (1970) 137.

161 I. Chen., Phys. Rev., B2 (1970) 1053.

162 I. Chen, Phys. Rev., B2 (1970) 1060.

163 H.C. Whitehead and G. Andermann, J. Phys. Chem., 77 (1973) 721.
164 W.R. Salaneck, N.O. Lipari, A. Paton, R. Zallen and K.S. Liang, Phys. Rev. B, 12 (1975) 1493.
165 W.R. Salaneck, C.B. Duke, A. Paton, C. Griffiths and R.C. Keezer, Phys. Rev. B, 15 (1977) 1100.
166 A. Datta, J. Mol. Struct., 92 (1983) 93.
167 M.J.S. Dewar and M.L. McKee, J. Comput. Chem., 4 (1983) 84.
168 N.C. Baird, J. Comput. Chem., 5 (1984) 35.
169 M.J.S. Dewar and C.H. Reynolds, J. Comput. Chem., 7 (1986) 140.
170 K. Jug and R. Iffert, J. Comput. Chem., 8 (1987) 1004.
171 A.B. Bolotin, P.P. Pipiraite, A. Yu. Ruzhene, N.B. Gorbunov, G.V. Tarkhov and L.B. Simanenkova, Zh. Strukt. Khim., 29 (1988) 19.
172 M.J.S. Dewar and Y.-C. Yuan, Inorg. Chem., 29 (1990) 3881.
173 H. Yilmaz and S. Erkoç, J. Mol. Struct. (Theochem), 231 (1991) 63.
174 R. Bini, P. Foggi, N.Q. Liem and P.R. Salvi, Chem. Phys. Lett., 151 (1988) 236.
175 S.H. Nilar, M.C. Zerner and R. Manne, Chem. Phys. Lett., 168 (1990) 260.
176 R. Boschi and W. Schmidt, Inorg. Nucl. Chem. Lett., 9 (1973) 643.
177 P. Nielsen, Phys. Rev. B, 10 (1974)1673.
178 N.V. Richardson and P. Weinberger, J. Electron Spectr. Relat. Phenom., 6 (1975) 109.
179 R. Steudel, D. Jensen, P. Göbel and P. Hugo, Ber. Bunsenges. Phys. Chem., 92 (1988) 118 and refs. therein.
180 D.R. Salahub, A.E. Foti and V.H. Smith Jr., J. Am. Chem. Soc., 100 (1978) 7847.
181 G.L. Carlson and L.G. Pedersen, J. Chem. Phys., 62 (1975) 4567.
182 K.D. Petri, A. MacKinnon, B. Kramer and P. Krusius, Solid State Commun., 36 (1980) 833.
183 M.H. Palmer and R.H. Findlay, Z. Naturforsch., 38a (1983) 1032.
184 M.H. Palmer, Z. Naturforsch., 38a (1983) 1359.
185 S. Itoh and K. Nakao, J. Phys. C, Solid State Phys., 17 (1984) 3373.
186 R.S. Laitinen, B. Randolph and T.A. Pakkanen, J. Comput. Chem., 8 (1987) 658.
187 D.A. Dixon and E. Wasserman, J. Phys. Chem., 94 (1990) 5772.
188 K. Raghavachari, C. McMichael Rohlfing and J.S. Binkley, Int. J. Mass Spectrosc. Ion Proc., 102 (1990) 313.
189 K. Raghavachari, C. McMichael Rohlfing and J.S. Binkley, J. Chem. Phys., 93 (1990) 5862.
190 K.S. Kim, J.H. Jang, S. Kim, B.-J. Mhin and H.F. Schaefer III, J. Chem. Phys., 92 (1990) 1887.
191 M.H. Palmer, Z. Naturforsch., 47a (1992) 203.
192 A. Hinchliffe, J. Mol. Struct., 55 (1979) 127.
193 C.J. Marsden and B.J. Smith, J. Mol. Struct., 105 (1983) 385.
194 S.W. Benson, Chem. Rev., 78 (1978) 23.
195 F.H. Stillinger, Physica A, 140 (1986) 142.
196 F.H. Stillinger, T.A. Weber and R. LaViolette, J. Chem. Phys., 85 (1986) 6460.
197 F.H. Stillinger and T.A. Weber, J. Phys. Chem., 91 (1987) 4899.
198 R.O. Jones, in K.P. Lawley, Ed., Ab Initio Methods in Quantum Chemistry – I, Wiley, 1987, p. 413.
199 D. Hohl and R.O. Jones, Ber. Kernforschungsanlage Juelich, JUEL-2336, 1989, 74 pp.
200 R.O. Jones and D. Hohl, 3rd Supercomput. Chem. IABG Workshop 1989, Berlin, 1990, p. 127.
201 R.O. Jones, Angew. Chem., 103 (1991) 647; Angew. Chem., Int. Ed. Engl., 30 (1991) 630.
202 R.O. Jones and D. Hohl, Phys. Scripta, T35 (1991) 154.
203 R.O. Jones and D. Hohl, Int. J. Quantum Chem., Quantum Chem. Symp., 24 (1990) 141.

204 C.M. Gramaccioli and G. Filippini, Chem. Phys. Lett., 108 (1984) 585.

205 E. Venutti, G. Cardini and E. Castellucci, Chem. Phys., 165 (1992) 313.

206 E. Venutti, P.R. Salvi and G. Cardini, J. Mol. Struct., 266 (1992) 229.

207 M.C. Chang, M.S. Jhon and H.Y. Kim, Bull. Korean Chem. Soc., 6 (1985) 29.

208 P.D. Harvey and I.S. Butler, J. Raman Spectrosc., 17 (1986) 329.

209 L. Wang, Y. Zhao, R. Lu, Y. Meng, Y. Fan, H. Luo, Q. Cui and G. Zou, in M.H. Manghnani and Y. Syono, Eds., High-Pressure Research in Mineral Physics, Terra Scientific, Tokyo 1987, p. 299.

210 P. Wolf, B. Baer, M. Nicol and H. Cynn, in R. Pucci and G. Piccitto, Eds., Molecular Systems under High Pressure, North-Holland, Amsterdam, 1991, p. 263.

211 K. Nagata, T. Nishio, H. Taguchi and Y. Miyamoto, Jpn. J. Appl. Phys., 31 (1992) 1078.

212 M. Schinazi, J. Corset, M. Delhaye and J.L. Lesne, Proc. 8th Int. Raman Spectrosc. Conf., 1982, p. 659.

213 P. Lenain, E. Picquenard, J. Corset, D. Jensen and R. Steudel, Ber. Bunsenges. Phys. Chem. 92 (1988) 859.

214 R.A. Zingaro and E.A. Meyers, Proc. Int. Symp. Ind. Uses Selenium Tellurium, 1980, p. 277.

215 I. Chen, Phys. Rev. B, 7 (1973) 3672.

216 I. Chen, Phys Rev. B, 11 (1975) 3976.

217 A. Ikawa and H. Fukutome, J. Phys. Soc. Jpn., 58 (1989) 4517.

218 D. Hohl, R.O. Jones, R. Car and M. Parrinello, Chem. Phys. Lett., 139 (1987) 540.

219 K. Nagata, T. Ishikawa and Y. Miyamoto, Jpn. J. Appl. Phys., 22 (1983) 1129.

220 K. Nagata, Y. Miyamoto, H. Nishimura, H. Suzuki and S. Yamasaki, Jpn. J. Appl. Phys., 24 (1985) L858.

221 J. Becker, K. Rademann and F. Hensel, Z. Phys. D, 19 (1991) 229.

222 J. Becker, K. Rademann and F. Hensel, Z. Phys. D, 19 (1991) 233.

223 J. Becker, K. Rademann and F. Hensel, Z. Naturforsch., 46a (1991) 453.

224 H.C.E. McFarlane and W. McFarlane, in J. Mason, Ed., Multinuclear NMR, Plenum Press, New York, 1986, p. 417.

225 R.S. Laitinen and T.A. Pakkanen, J. Chem. Soc., Chem. Commun., (1986) 1381.

226 R.S. Laitinen and T.A. Pakkanen, Inorg. Chem., 26 (1987) 2598.

227 T. Chivers, R.S. Laitinen and K.J. Schmidt, Can. J. Chem., 70 (1992) 719.

228 R. Laitinen and R. Steudel, J. Mol. Struct., 68 (1980) 19.

229 H.H. Eysel, J. Mol. Struct., 78 (1982) 203.

230 H.H. Eysel and S. Sunder, Ind. J. Chem., 18A (1979) 447.

231 R. Frey and H.H. Eysel, Z. Anorg. Allg. Chem., 489 (1982) 173.

232 A. Datta and V. Khrishnan, Ind. J. Chem., 16A (1978) 335.

233 P. Pekonen, Y. Hiltunen, R.S. Laitinen and T.A. Pakkanen, Inorg. Chem., 30 (1991) 3679.

234 H. Eggert, O. Nielsen and L. Henriksen, J. Am. Chem. Soc., 108 (1986) 1725.

235 H.C.E. McFarlane and W. McFarlane, J. Chem. Soc., Dalton Trans., (1973) 2416.

236 M. Binneweiss, Z. Anorg. Allg. Chem. 422 (1976) 43.

237 C.H.W. Jones and M. Mauguin, J. Chem. Phys., 67 (1977) 1587.

238 R. Steudel and F. Schuster, J. Mol. Struct., 44 (1978) 143.

239 K. Jug and R. Iffert, J. Mol. Struct. (Theochem), 186 (1989) 347.

240 T. Takahashi, S. Yagi, T. Sagawa, K. Nagata and Y. Miyamoto, J. Phys. Soc. Jpn., 54 (1985) 1018.

241 R.J. Suontamo, R.S. Laitinen and T.A. Pakkanen, Acta Chem. Scand., 45 (1991) 687.

242 R.O. Jones and D. Hohl, J. Am. Chem. Soc., 112 (1990) 2590.

243 R. Laitinen, R. Steudel and E.-M. Strauss, J. Chem. Soc., Dalton Trans., (1985) 1869.

244 R. Steudel, M. Papavassiliou, D. Jensen and K. Seppelt, Z. Naturforsch., 43b (1988) 245.

245 R.S. Laitinen and T.A. Pakkanen, J. Mol. Struct., 108 (1984) 263.
246 R.P. Fraser, G. Boussard, J.K. Saunders, J.B. Lambert and C.E. Mixan, J. Am. Chem. Soc., 93 (1971) 3822.
247 R. Steudel, Z. Naturforsch., 38b (1983) 543.
248 R. Steudel, M. Papavassiliou and W. Krampe, Polyhedron, 7 (1988) 581.
249 P. Pekonen, Y. Hiltunen, R.S. Laitinen, and J. Valkonen, Inorg. Chem., 30 (1991) 1874.
250 L.A. Nimon, V.D. Neff, R.E. Cantley and R.O. Buttlar, J. Mol. Spectrosc., 22 (1967) 105.
251 L.A. Nimon and V.D. Neff, J. Mol. Spectrosc., 26 (1968) 175.
252 J. Berkowitz, W.A. Chupka, E. Bromels and R.L. Belford, J. Chem. Phys., 47 (1967) 4320.
253 R. Steudel, Spectrochim. Acta, A31 (1975) 1065.
254 K. Nagata, K. Ishibashi and Y. Miyamoto, Jpn. J. Appl. Phys., 19 (1980)1569.
255 K. Nagata, K. Ishibashi and Y. Miyamoto, Jpn. J. Appl. Phys., 20 (1981) 463.
256 Y. Xie, H.F. Schaefer III, J.H. Jang, B.J. Mhin, H.S. Kim, C.W. Yoon and K.S. Kim, Mol. Phys., 76 (1992) 537.
257 Z.S. Herman and K. Weiss, Inorg. Chem., 14 (1975) 1592.
258 N.L. Allinger, M.J. Hickey and J. Kao, J. Am. Chem. Soc., 98 (1976) 2741.
259 R.C. Burns, M.J. Collins, S.M. Eicher, R.J. Gillespie and J.F. Sawyer, Inorg. Chem., 27 (1988) 1807.
260 T. Takahashi, K. Murano, K. Nagata and Y. Miyamoto, Phys. Rev. B, 28 (1983) 4893.
261 N.R. Carlsen and H.F. Schaefer III, Chem. Phys. Lett., 48 (1977) 390.
262 W.L. Feng and O. Novaro, Int. J. Quantum Chem., 26 (1984) 521.
263 W.L. Feng, O. Novaro and J. Carcia-Prieto, Chem. Phys. Lett., 111 (1984) 297.
264 J.E. Rice, R.D. Amos, N.C. Handy, T.J. Lee and H.F. Schaefer III, J. Chem. Phys., 85 (1986) 963.
265 N.C. Baird, J. Mol. Struct. (Theochem), 137 (1986) 1.
266 W. von Niessen and P. Tomasello, J. Chem. Phys., 87 (1987) 5333.
267 T. Fueno and R.J. Buenker, Theor. Chim. Acta, 73 (1988)123.
268 J.K. Burdett and C.J. Marsden, New. J. Chem., 12 (1988) 797.
269 H. Basch, Chem. Phys. Lett., 157 (1989) 129.
270 M. Morin, A.E. Foti and D.R. Salahub, Can. J. Chem., 63 (1985) 1982.
271 R.O. Jones, J. Chem. Phys., 84 (1986) 318.
272 A.A. Bhattacharyya, A. Bhattacharyya, R.R. Adkins and A.G. Turner, J. Am. Chem. Soc., 103 (1981) 7458.
273 W.G. Laidlaw and M. Trsic, Chem. Phys., 36 (1979) 323.
274 W.G. Laidlaw and M. Trsic, Can. J. Chem., 63 (1985) 2044.
275 W. von Niessen, L.S. Cederbaum and F. Tarantelli, J. Chem. Phys., 91 (1989) 3582.
276 B. Meyer, T.V. Oommen and D. Jensen, J. Phys. Chem., 75 (1971) 912.
277 B. Meyer, T. Stroyer-Hansen and T.V. Oommen, J. Mol. Spectrosc., 42 (1972) 335.
278 H.L. Casal and J.C. Scaiano, J. Photochem., 30 (1985) 253.
279 J. Berkowitz and C. Lifshitz, J. Chem. Phys., 48 (1968) 4346.
280 W. Rosinger, M. Grade and W. Hirschwald, Ber. Bunsenges. Phys. Chem., 87 (1983) 536.
281 M.R. Nimlos and G.B. Ellison, J. Phys. Chem., 90 (1986) 2574.
282 S.-Y. Tang and C.W. Brown, Inorg. Chem., 14 (1975) 2856.
283 P. Lenain, E. Picquenard, J.L. Lesne and J. Corset, J. Mol. Struct., 142 (1986) 355.
284 H. Schnöckel, H.-J. Göcke and R. Elsper, Z. Anorg. Allg. Chem., 494 (1982) 78.
285 G.D. Brabson, Z. Mielke and L. Andrews, J. Phys. Chem., 95 (1991) 79.
286 J. Kao, Inorg. Chem., 16 (1977) 2085.
287 A.E. Foti, V.H. Smith and D.R. Salahub, Chem. Phys. Lett., 57 (1978) 33.
288 A.F. Cuthbertson and C. Glidewell, Inorg. Chim. Acta, 49 (1981) 91.

289 G.E. Quelch, H.F. Schaefer III and C.J. Marsden, J. Am. Chem. Soc., 112 (1990) 8719.
290 W. von Niessen, J. Chem. Phys., 95 (1991) 8301.
291 L.J. Saethre and O. Gropen, Can. J. Chem., 70 (1992) 348.
292 B. Meyer and T. Stroyer-Hansen, J. Phys. Chem., 76 (1972) 3968.
293 R. Steudel, J. Albertsen and K. Zink, Ber. Bunsenges. Phys. Chem., 93 (1989) 502.
294 E.-M. Strauss and R. Steudel, Z. Naturforsch., 42b (1987) 682.
295 W. Genz and P.W. Schenk, Z. Anorg. Allg. Chem., 379 (1970) 300.
296 J. Kao, Inorg. Chem., 16 (1977) 3347.
297 R. Steudel and M. Rebsch, J. Mol. Spectrosc., 51 (1974) 189.
298 R. Steudel and H.-J. Mäusle, Z. Naturforsch., 33a (1978) 951.
299 K.S. Kim, H.S. Kim, S. Kim, J.H. Jang and H.F. Schaefer III, J. Am. Chem. Soc., 111 (1989) 7746.
300 R.O. Jones, J. Chem. Phys., 82 (1985) 325.
301 E.T. Seidl and H.F. Schaefer III, J. Chem. Phys., 88 (1988) 7043.
302 C.P. Blahous and H.F. Schaefer III, J. Phys. Chem., 92 (1988) 959.
303 D. Hohl, R.O. Jones, R. Car and M. Parrinello, J. Am. Chem. Soc., 111 (1989) 825.
304 R. Steudel and H.-J. Mäusle, Angew. Chem., 89 (1977) 114; Angew. Chem., Int. Ed. Engl., 16 (1977) 112.
305 H.-J. Mäusle and R. Steudel, Z. Anorg. Allg. Chem., 478 (1981) 177.
306 R. Steudel, Z. Anorg. Allg. Chem., 478 (1981)139.
307 R. Steudel, H.-J. Mäusle, D. Rosenbauer, H. Möckel and T. Freyholdt, Angew. Chem., 93 (1981) 402; Angew. Chem., Int. Ed. Engl., 20 (1981) 394.
308 H.J. Möckel, T. Freyholdt, J. Weiss and I. Molnar, in I. Molnar, Ed., Pract. Aspects Mod. High Perform. Liq. Chromatogr., Proc. 1981, de Gruyter, Berlin, 1983, p. 161.
309 H.J. Möckel, Fresenius Z. Anal. Chem., 318 (1984) 327.
310 R. Strauss and R. Steudel, Fresenius Z. Anal. Chem., 326 (1987) 543.
311 R. Steudel and E.-M. Strauss, Z. Naturforsch., 36b (1981) 1085.
312 R. Steudel, R. Strauss and L. Koch, Angew. Chem., 97 (1985) 58; Angew. Chem., Int. Ed. Engl., 24 (1985) 59.
313 J. Harris and R.O. Jones, Phys. Rev. A, 19 (1979) 1813.
314 R. Steudel, E.-M. Strauss and D. Jensen, Z. Naturforsch., 45b (1990) 1282.
315 R. Steudel, S. Passlack-Stephan and G. Holdt, Z. Anorg. Allg. Chem., 517 (1984) 7.
316 R. Steudel and R. Strauss, Z. Naturforsch., 37b (1982) 1219.
317 I. Kende, T.L. Pickering and A.V. Tobolsky, J. Am. Chem. Soc., 87 (1965) 5582.
318 T.L. Pickering, K.J. Saunders and A.V. Tobolsky, J. Am. Chem. Soc., 89 (1967) 2364.
319 M. Porter, in B. Zwanenburg and A.J.H. Klunder, Eds., Perspectives in Organic Chemistry of Sulfur, Elsevier, Amsterdam,1987, p. 267.
320 F.N. Tebbe, E. Wasserman, W.G. Peet, A. Vatvars and A.C. Hayman, J. Am. Chem. Soc., 104 (1982) 4971.
321 D.M. Gardner and G.F. Fraenkel, J. Am. Chem. Soc., 78 (1956) 3279
322 D.C. Koningsberger and T. Neef, Chem. Phys. Lett., 4 (1970) 615.
323 D.C. Koningsberger and T. Neef, Chem. Phys. Lett., 14 (1972) 453.
324 R. Steudel, J. Non-Cryst. Solids, 83 (1986) 63.
325 R.L. Kucczkowski and E.B. Wilson, J. Am. Chem. Soc., 85 (1963) 2028.
326 M. Feuerhahn and G. Vahl, Chem. Phys. Lett., 65 (1979) 322.
327 B.M. Chadvick, J.M. Grzybowski and D.A. Long, J. Mol. Struct., 48 (1978) 139.
328 D.N. Harpp, K. Steliou and C.J. Cheer, J. Chem. Soc., Chem. Commun., (1980) 825.
329 N.C. Baenzinger, R.E. Buckles, R.J. Maner and T.D. Simpson, J. Am. Chem. Soc., 91 (1969) 5749.

330 G.E. Wilson and M.M.Y. Chang, Tetrahedron Lett., (1971) 875.
331 A. Haas and H. Willner, Z. Anorg. Allg. Chem., 462 (1980) 57.
332 R.A. Hayes and J.C. Martin, in I.G. Csizmadia, A. Mangini and F. Bernardi, Eds., Organic Sulfur Chemistry: Theoretical and Experimental Advances, Elsevier, Amsterdam 1985, p. 1.
333 R.S. Laitinen, T.A. Pakkanen and R. Steudel, J. Am. Chem. Soc., 109 (1987) 710.
334 R. Steudel, Phosphorus Sulfur, 16 (1983) 251.
335 D.N. Harpp, in B. Zwanenburg and A.J.H. Klunder, Eds., Perspectives of Organic Chemistry of Sulfur, Elsevier, Amsterdam 1987, p. 1.
336 G.W. Kutney and K. Turnbull, Chem. Rev., 82 (1982) 333.
337 W.M. Tolles and W.D. Gwinn, J. Chem. Phys., 36 (1962) 1119.
338 K. Kimura and S.H. Bauer, J. Chem. Phys., 39 (1963) 3172.
339 J. Geyer, H. Stülpnagel and K. Rademan, Angew. Chem., 104 (1992) 894; Angew. Chem., Int. Ed. Engl., 31(1992) 874.
340 N.Z. Boctor and G. Kullerud, J. Solid State Chem., 71 (1987) 513.
341 W.E. Ringer, Z. Anorg. Chem., 32 (1902) 183.
342 R. Steudel, G. Holdt and A.T. Young, J. Geophys. Res., 91(1986) 4971.